Reactions of Cyclic Aliphatic and Aromatic Amines on Ge(100)-2×1 and Si(100)-2×1

George T. Wang,[†] Collin Mui,[†] John F. Tannaci,[†] Michael A. Filler,[†] Charles B. Musgrave,[†,‡] and Stacey F. Bent*[,†]

Department of Chemical Engineering, Stanford University, Stanford, California 94305-5025, and Department of Materials Science and Engineering, Stanford University, Stanford, California 94305-2205

Received: August 28, 2002; In Final Form: February 10, 2003

We have examined the reaction of the Ge(100)-2×1 surface with five-membered cyclic amines including pyrrolidine, 3-pyrroline, pyrrole, and their *N*-methyl-capped analogues. The reactions of pyrrolidine, *N*-methylpyrrolidine, pyrrole, and *N*-methylpyrrole were also probed on the Si(100)-2×1 surface for comparison. Multiple internal reflection (MIR) infrared spectroscopy in combination with density functional theory (DFT) cluster calculations were used to study the reactions. We find that for the aliphatic amines, dative bonding of the N lone pair to the electrophilic down atom of the surface dimer competes with N−H dissociation and [2 + 2] cycloaddition to form stable surface adducts at room temperature and is the major surface reaction observed on the Ge(100) surface. At higher coverages, some evidence for N−H dissociation is seen on the Ge(100) surface. For pyrrole and *N*-methylpyrrole, the aromatic system of π electrons is seen to have profound effects on their reactivity with the Si(100) and Ge(100) surfaces. The delocalized system of π electrons allows a kinetically favored alternative pathway for N−H dissociation via dative bonding at a ring carbon, resulting in the facile N−H dissociation of pyrrole on the Ge(100) surface, in contrast to the case for aliphatic amines. Evidence is obtained suggesting that pyrrole and *N*-methylpyrrole also undergo electrophilic aromatic substitution reactions at the surfaces, reactions that have not been previously observed for benzene and other aromatic molecules. We have also compared the known reactivity of pyrrole with its reactivity on Si(100) and Ge(100) and have found interesting similarities, demonstrating that principles used to understand the chemistry of organic molecules can also be applicable and useful for understanding bonding at semiconductor surfaces.

I. Introduction

Over the past several years, there has been a surge of interest in the covalent attachment of organic molecules to the surfaces of group IV semiconductors including silicon, germanium, and diamond. This interest has been driven in part by the expectation that the organic modification, or "functionalization," of semiconductors will have technological applications in the future. Although the number of studies examining the adsorption behavior of a variety of organic molecules on clean semiconductor surfaces has been growing steadily over time, the factors and principles that control reactivity and selectivity on semiconductor surfaces, as well as the differences in reactivity between different semiconductors, are not fully understood.

Recent studies of the reaction of a series of ketones on the Si(100) and Ge(100) surfaces have found that selectivity is significantly enhanced on the Ge(100)-2×1 surface.[1] Because selectivity is one of the most difficult issues in functionalizing clean semiconductor surfaces with organics, this study indicated that the Ge(100)-2×1 surface might be a superior material for the attachment of multifunctional organics. However, the number of studies of organic surface chemistry on Ge(100)-2×1 that have been carried out to date is small relative to those on Si(100)-2×1.

If the Ge(100)-2×1 surface is to be used as a semiconductor substrate for the selective attachment of organics, it will be necessary to gain an improved understanding of how various classes of organic molecules react with the Ge(100)-2×1 surface. In this work, we have investigated the adsorption of a series of aliphatic and aromatic five-membered cyclic amines (Figure 1) including pyrrolidine, *N*-methylpyrrolidine, 3-pyrroline, *N*-methyl-3-pyrroline, pyrrole, and *N*-methylpyrrole on the Ge(100)-2×1 surface. The adsorption of all of the amines except for 3-pyrroline and *N*-methyl-3-pyrroline was also probed on the Si(100)-2×1 surface and compared to the Ge(100) results. All reactions were investigated using multiple internal reflection (MIR) infrared spectroscopy and density functional theory (DFT) cluster calculations, which we have demonstrated in previous studies to be a powerful combination for probing the chemistry of organics with semiconductor surfaces.[1−6]

Except for alkenes, amines have probably been the most studied group of organic molecules on clean semiconductor surfaces, specifically, the Si(100)-2×1 surface. Much has been learned about the N−H dissociation reactions of primary and secondary amines on the Si(100)-2×1 surface,[3,4,6−18] and the stable dative bonding of tertiary amines has been reported on Si(100)-2×1.[3,4,17] To our knowledge, however, the only amines whose reactivity has been previously probed on Ge(100)-2×1 are a series including methylamine, dimethylamine, and trimethylamine.[6]

By systematically studying the reaction of a related group of amines whose functionality increases from pyrrolidine to 3-pyrroline to pyrrole along with their *N*-methyl-capped analogues, it is hoped that valuable insight into the mechanisms of different surface reactions as well as the competition between

* Corresponding author. E-mail: stacey.bent@stanford.edu.
† Department of Chemical Engineering.
‡ Department of Materials Science and Engineering.

10.1021/jp026864j CCC: $25.00
Published on Web 05/02/2003

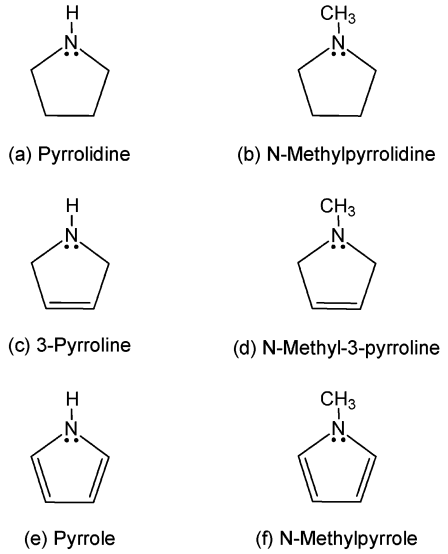

Figure 1. Series of five-membered cyclic amines studied in present work.

reactions on both the Si(100)-2×1 and Ge(100)-2×1 surfaces will be gained. Additionally, by comparing the surface reactivity of pyrrole and *N*-methylpyrrole to that of the aliphatic amines in this study, the effects of aromaticity on the surface chemistry can be investigated. Figure 2 shows several possible reactions that pyrrole and *N*-methylpyrrole can undergo with the Si(100) and Ge(100) surfaces; the other molecules can undergo a subset of these reactions.

II. Experimental Details and Theoretical Methods

Experiments were performed in an ultrahigh vacuum (UHV) chamber that has previously been described in detail.[19] Infrared data were collected in multiple internal reflection (MIR) mode using a Fourier transform infrared (FTIR) spectrometer with a narrow-band HgCdTe detector. For each experiment, the IR emissivity of the clean sample was recorded as the background spectrum, and the ratios of subsequent IR spectra of the sample after exposure to gas-phase molecules to this background spectrum were used to transform the emissivity spectra to absorption spectra. The absorption spectra have been corrected for baseline instabilities using the "multipoint" method, in which straight-line segments are subtracted from the uncorrected absorption spectra over discrete regions of the spectra. The samples, Ge(100) and Si(100) crystals of trapezoidal geometry ($1 \times 20 \times 50$ mm, 45° beveled edges), were conductively heated by a resistive tungsten heater and cooled by heat exchange with a liquid nitrogen coldfinger. The sample surfaces were cleaned by sputtering with Ar^+ ions at room temperature followed by annealing to 875 K for 4 min for Ge(100) and 1050 K for ~1 min for Si(100). The back faces of the crystals, which are not cleaned by sputtering, were covered with a thin molybdenum plate to prevent adsorption at those surfaces.

Pyrrolidine (99% purity, Lancaster Synthesis), *N*-methylpyrrolidine (98% purity, Fisher Scientific), 3-pyrroline (97% purity, Lancaster Synthesis), pyrrole (99% purity, Fisher Scientific), pyrrole-2,3,4,5-d_4 (98% D purity, CDN Isotopes), and *N*-methylpyrrole (99+% purity, Fisher Scientific) were transferred to sample vials in a nitrogen-purged glovebag and further purified by repeated freeze−pump−thaw cycles before introduction into the chamber through a variable leak valve. All exposures were performed by filling the chamber with the compound for a given pressure and time and are reported in units of langmuir ($1\ L = 1 \times 10^{-6}$ Torr s). The pressures have not been corrected for ion gauge sensitivity. Saturation exposures were achieved when subsequent doses did not result in an increase in IR intensity and represent upper limits necessary to achieve saturation for the different systems. *N*-methyl-3-pyrroline was dosed in the same manner after it was synthesized using the following procedure: *cis*-1,4-Dichlorobut-2-ene (10 g) was added dropwise over 2 h to a stirred solution of aqueous methylamine (70 mL, 40 wt %). DMF (a few milliliters) was added to ensure a single phase as mixing began. The resulting solution was stirred overnight, made basic with 1 M NaOH, and extracted with cyclopentane. The extract was dried ($MgSO_4$) and distilled. The clear, colorless fraction at 55 °C (cyclopentane and *N*-methyl-3-pyrroline in a 5:1 ratio) was collected and used in the UHV chamber: ^{1}H NMR in $CDCl_3$: δ 2.52 (3 H, s, methyl), 3.51 (4 H, d, sp^3 ring C), 5.76 (2 H, t, sp^2 ring C).

Our theoretical approach is based on density functional theory (DFT)[20,21] with the electronic structure expanded in atomic Gaussian basis functions. The Si(100)-2×1 surface is modeled by a Si_9H_{12} one-dimer cluster consisting of four layers of silicon atoms, with the two Si atoms in the top layer comprising the surface dimer. To model the Ge(100)-2×1 surface, the top two Si atoms of the Si one-dimer cluster were replaced with Ge atoms, resulting in the $Ge_2Si_7H_{12}$ cluster model (Figure 3). A full nine-atom Ge_9H_{12} Ge cluster was not used because of the computational expense required, except for comparison purposes to check the validity of using the $Ge_2Si_7H_{12}$ cluster. We find that for pyrrolidine the calculated energies using the full nine-atom Ge cluster are approximately 1 kcal/mol more stable than those using the $Ge_2Si_7H_{12}$ cluster. Previous calculations of the [4 + 2] and [2 + 2] cycloaddition reactions of 1,3-butadiene on Ge(100)-2×1 using B3LYP have found that using a $Ge_2Si_7H_{12}$ cluster to model the Ge surface rather than the full Ge_9H_{12} cluster results in less than a 2 kcal/mol difference in the calculated binding (adsorption) energies (which are weaker on $Ge_2Si_7H_{12}$).[22] Hence, we expect this approach to be acceptable for modeling the present system.

We note that one-dimer cluster models may not adequately capture charge-transfer effects at the surface, which can stabilize dative-bonded products through delocalization of charge to unoccupied sites on adjacent dimers in the same row. These effects have been theoretically examined in detail on the Si(100)-2×1 surface by Widjaja et al., who reported that ammonia dative-bonded to the center dimer of an unoccupied three-dimer Si(100)-2×1 cluster is calculated to be lower in energy by ~6 kcal/mol versus ammonia dative-bonded to a one-dimer Si_9H_{12} cluster.[23] The magnitude of charge-transfer delocalization effects on the Ge(100)-2×1 surface have not been previously examined to our knowledge. The numbers reported in this paper have not been corrected for any charge-transfer effects.

All calculations in this work were made using the Gaussian 98 software package.[24] The BLYP/6-31G(d) level of theory[25,26] was used to determine the geometries of the critical points on the potential energy surface. Structures were fully optimized without geometrical constraints on the clusters, and symmetry restrictions were applied where appropriate. Single-point energy calculations were performed on the optimized structures at the B3LYP level of theory[26,27] with a mixed basis set scheme to minimize computational costs. The mixed basis set scheme uses the 6-311++G(d,p) basis set to describe the chemically active surface dimer atoms and the amine adsorbate and the smaller 6-31G(d) basis set to describe the subsurface atoms and terminating hydrogens. The reported energies have been zero-point corrected. All calculated minima and transition states on

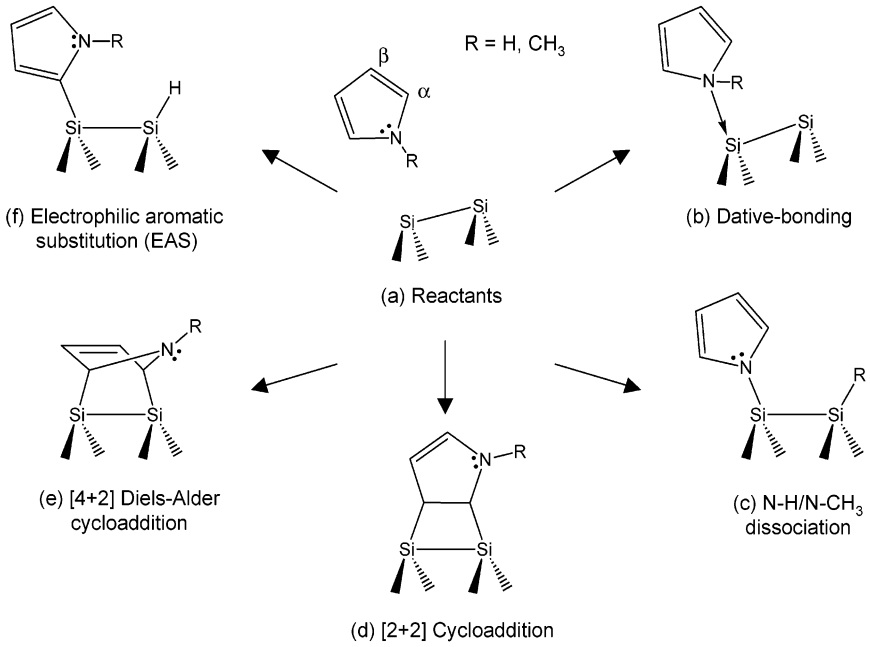

Figure 2. Possible reaction pathways for pyrrole and *N*-methylpyrrole on Si(100)-2×1 and Ge(100)-2×1: (a) Reactants. Products of (b) dative bonding. (c) N−H/N−CH_3 dissociation. (d) [2 + 2] cycloaddition. (e) [4 + 2] Diels−Alder cycloaddition. (f) Electrophilic aromatic substitution.

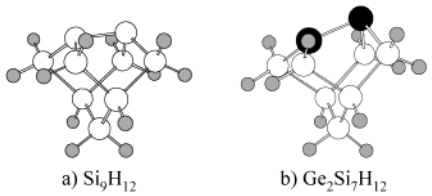

Figure 3. One-dimer clusters used to model the Si(100)-2×1 and Ge(100)-2×1 surfaces: (a) Si_9H_{12} cluster model. (b) $Ge_2Si_7H_{12}$ cluster model.

the potential energy surfaces have been verified by frequency calculations to have zero and only one imaginary frequency, respectively. Previous studies of amines on Si(100)-2×1 and Ge(100)-2×1 using this theoretical approach have been shown to give results that are consistent with experimental observations.[3,4,6]

III. Results

A. Pyrrolidine. Pyrrolidine is a saturated secondary amine that in previous studies has been found to undergo N−H dissociation with the clean Si(100)-2×1 surface at room temperature.[3,11,28] The IR spectra of the Si(100)-2×1 and Ge(100)-2×1 surfaces after saturation doses of pyrrolidine at room temperature are shown in Figure 4. The physisorbed or "multilayer" spectrum of pyrrolidine at 115 K is also shown in Figure 4c for comparison because it represents the unreacted molecular spectrum of pyrrolidine. Following the exposure of the Si(100)-2×1 surface to pyrrolidine at room temperature, a complete loss of the N−H stretching mode at 3190 cm^{-1} in Figure 4c can be seen together with the appearance of a Si−H stretching mode at 2070 cm^{-1} in Figure 4a. The IR data indicate dissociative chemisorption of pyrrolidine to Si(100) through cleavage of the N−H bond, forming a surface Si−H bond in the process, as previously reported.[3,11,28] The negative dip at 2091 cm^{-1} in Figure 4a has been previously addressed in detail and is the likely result of some preexisting surface hydrogen that has been shifted upon pyrrolidine adsorption.[3]

On Ge(100), in contrast to Si(100), a significant ν(N−H) mode at ∼3190 cm^{-1} is observed after a saturation dose of

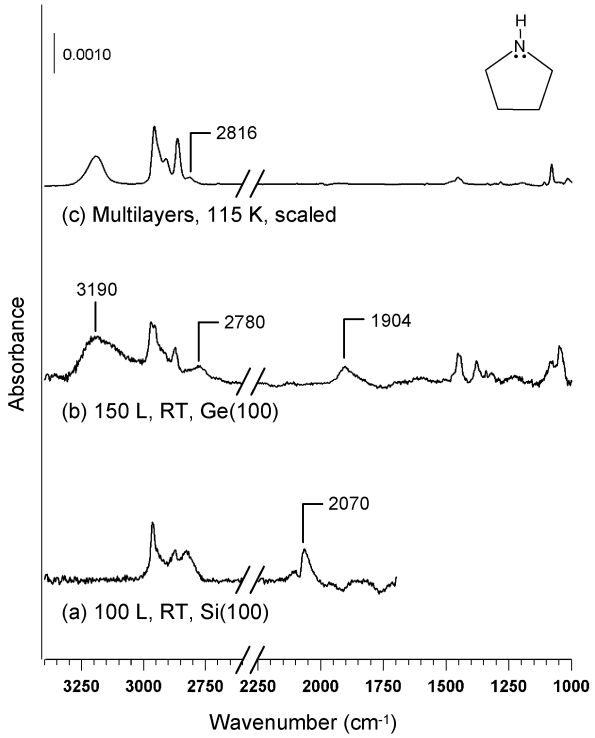

Figure 4. Infrared spectra of pyrrolidine on the Si(100)-2×1 and Ge(100)-2×1 surfaces: (a) 100 L at 298 K on Si(100). (b) 150 L at 298 K on Ge(100). (c) Multilayers (scaled to fit the Figure) at 117 K.

pyrrolidine, as shown in Figure 4b. Saturated alkanes have never been reported to chemisorb to clean semiconductor surfaces at room temperature (e.g., through C−H dissociation). We have also verified that cyclopentane, the saturated alkane analogue of pyrrolidine, does not react with the Ge(100) surface at room temperature (not shown). Thus, the adsorption of pyrrolidine most likely involves the N−H group. The retention of the ν(N−H) mode thus suggests that pyrrolidine dative-bonds to the Ge(100) surface through the nitrogen lone pair because this adduct would still have its N−H bond intact. Similarly, Mui et al. have found that methylamine and dimethylamine also

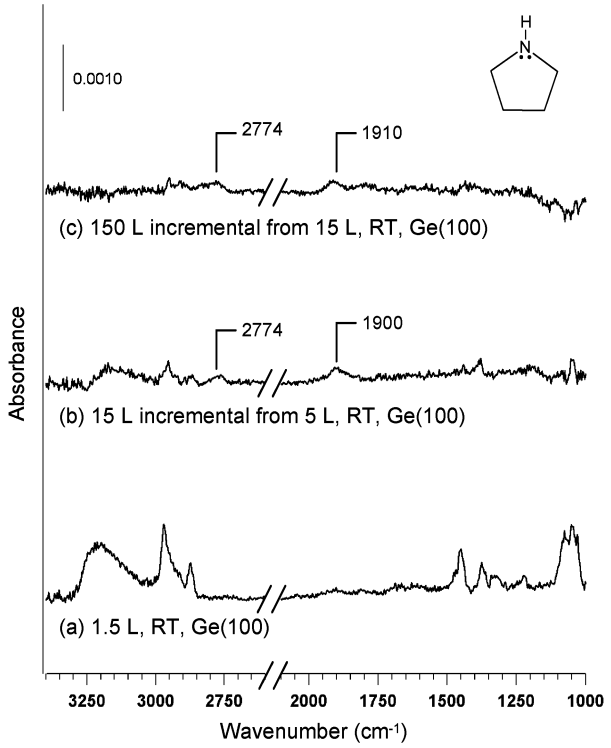

Figure 5. Infrared spectra of pyrrolidine on the Ge(100)-2×1 surface with increasing exposure: (a) 1.5 L at 298 K. (b) 15 L, in ratio with 1.5 L at 298 K. (c) 150 L, in ratio with 15 L at 298 K.

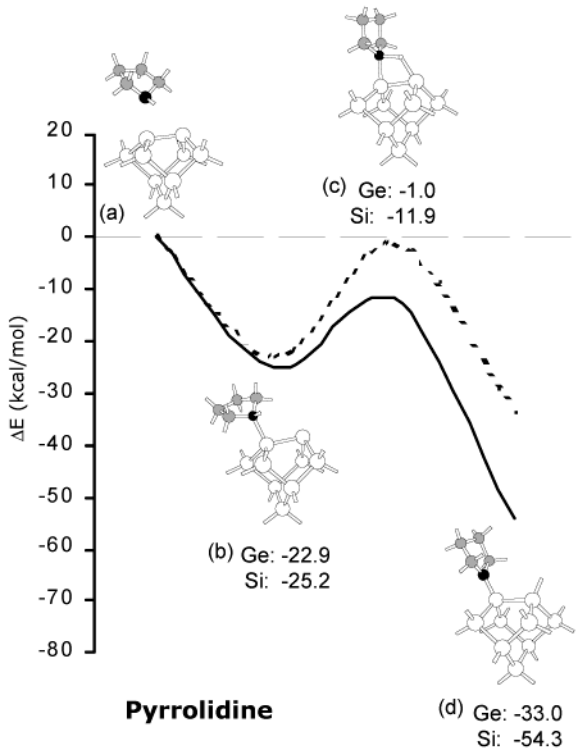

Figure 6. Critical points on the potential energy surfaces of the N−H dissociation reaction of pyrrolidine on the Si(100)-2×1 and Ge(100)-2×1 surfaces: (a) Reactants. (b) Dative-bonded precursor. (c) Transition state. (d) N−H dissociated product.

undergo dative bonding with the Ge(100)-2×1 surface rather than the proton-transfer reaction (i.e., N−H dissociation) that is observed on the Si(100)-2×1 surface.[6]

Whereas the ν(N−H) mode on Ge(100) indicates dative-bonded pyrrolidine species, a peak in the ν(Ge−H) stretching region at 1904 cm^{-1} is also present, which suggests the presence of some N−H dissociation adducts as well. An examination of the coverage-dependent adsorption behavior of pyrrolidine on Ge(100) indicates that N−H dissociation occurs only at higher coverages, with the initial adsorption occurring through dative bonding. Figure 5 shows difference spectra following *incremental* exposures (i.e., in ratio to the previous exposure) of Ge(100) to 1.5, 15, and 150 L of pyrrolidine. After an initial 1.5-L exposure of pyrrolidine on the clean Ge(100)-2×1 surface (Figure 5a), significant growth of peaks is seen, including a large N−H mode. However, no significant ν(Ge−H) mode near 1900 cm^{-1} can be observed. Additionally, there is no evidence at 1.5 L for the low-wavenumber Bohlmann band seen in the multilayer spectrum at ∼2816 cm^{-1} in Figure 4c and ∼2780 cm^{-1} after a saturation exposure on Ge(100) in Figure 4b. This Bohlmann band arises from the interaction of the N lone pair with trans-periplanar C−H bonds,[29,30] and its absence in Figure 5a indicates that the lone pair is directly involved in bonding (i.e., dative bonding).

Figure 5b shows the spectral change following an incremental dose of pyrrolidine from an exposure of 1.5 L to a total of 15 L on Ge(100). Although some intensity grows in over the N−H stretch, indicating the growth of additional dative-bonded species, both a Bohlmann band at 2774 cm^{-1} and a ν(Ge−H) mode at ∼1900 cm^{-1} are now also observed, indicating that some N−H dissociation has occurred after the 15-L exposure. Of note is the anomalously low position of the ν(Ge−H) mode, which is known to occur at 1979 and 1991 cm^{-1} on the Ge(100)-2×1 monohydride surface[31] and at 1967 cm^{-1} for the ene product of acetone on Ge(100)-2×1.[5] We believe that the large red shift of the ν(Ge−H) mode is due to the presence of adjacent dative-bonded pyrrolidine species. Queeney et al. recently calculated a large red shift in the ν(Si−H) mode of 62 cm^{-1} when Si−H is adjacent to a dative-bonded ammonia species on the neighboring dimer (in the same row) of the Si(100)-2×1 surface.[32] The red-shifted peak was not observed in their study, however, because dative-bonded species are not present in sufficient concentration on Si(100). Finally, after an incremental exposure of pyrrolidine from 15 to 150 L (Figure 5c), only slight additional adsorption is seen, which appears to occur completely through N−H dissociation, as indicated by the growth of the ν(Ge−H) peak and the lack of growth of the ν(N−H) peak. Furthermore, we can rule out the possibility that a fixed fraction of pyrrolidine dissociates at all coverages and is merely below the detection limit at low coverages. If a constant fraction were formed, then the ratio of the C−H and Ge−H IR absorption intensities would be constant in the incremental IR spectra. However, the Ge−H intensity clearly grows in larger proportion in the incremental spectra. Hence, we conclude that the reaction of pyrrolidine with the Ge(100)-2×1 surface at lower coverages is through dative bonding and that N−H dissociation occurs only at high coverages.

We have calculated the critical points on the potential energy surfaces, shown in Figure 6, for the reaction of pyrrolidine on Si(100)-2×1 and Ge(100)-2×1. The substantially weaker binding (adsorption) energy of the N−H dissociated product on Ge versus Si is due to the weaker organometallic bonds that the Ge surface forms and has been calculated or observed for a number of other systems as well.[1,5,6,33−37] We have also calculated a substantial difference in the barriers for N−H dissociation on the two surfaces. Whereas the calculated transition state for N−H dissociation on Si(100) is located 11.9 kcal/mol below the energy of the reactants, on Ge(100) the

transition state is calculated to be only 1 kcal/mol below the energy of the reactants. If pyrrolidine is accommodated in the precursor state (i.e., energy is lost to the surface), then this difference in barriers may explain why on Si(100) pyrrolidine undergoes complete N−H dissociation[3,11,28] whereas on Ge(100) a majority of pyrrolidine molecules are trapped in the dative-bonded precursor state.

Because Mui et al. recently reported that methylamine and dimethylamine are trapped in their dative bonding states on Ge(100) with no evidence of significant N−H dissociation,[6] the observation of significant N−H dissociation for pyrrolidine on Ge(100) at high coverages is of interest. Using the same level of theory and a full Ge_9H_{12} one-dimer cluster, the transition state of pyrrolidine is calculated to be 1.9 kcal/mol below the energy of the reactants, whereas for dimethylamine the transition state has previously been calculated to lie 0.1 kcal/mol above the energy of the reactants.[6] These calculated differences in the location of the transition states for N−H dissociation, although slight, may be sufficient to explain why proton transfer occurs for pyrrolidine and not dimethylamine. We are uncertain as to why high coverage appears to facilitate the proton transfer of pyrrolidine on Ge(100). It may be that the presence of neighboring dative-bonded species lowers the barrier for N−H dissociation, although we have not examined theoretically the adsorption of pyrrolidine on Ge(100)-2×1 using a multidimer cluster.

To summarize the results of the pyrrolidine studies, pyrrolidine undergoes total N−H dissociation on the Si(100) surface, whereas on Ge(100) the molecule adsorbs primarily to form a dative-bonded adduct at room temperature. At higher coverages, evidence is seen for some N−H dissociation on Ge(100).

B. *N*-Methylpyrrolidine. We have also previously studied the adsorption of *N*-methylpyrrolidine on the Si(100)-2×1 surface to determine the effect of capping the nitrogen of pyrrolidine with a methyl group.[3] The results are summarized here. It was found that *N*-methylpyrrolidine is stably trapped in a dative-bonded state at room temperature on Si(100) because the barriers for dissociation of the methyl group and for desorption from the dative-bonded state are prohibitive. The IR spectrum of a saturation dose of *N*-methylpyrrolidine on the Si(100) surface at room temperature is shown in Figure 7a. The loss of the strong Bohlmann bands of *N*-methylpyrrolidine below 2800 cm^{-1}, which are evident in the multilayer spectrum of the compound shown in Figure 7c, indicates that the N lone pair is directly involved in bonding with the Si(100) surface (i.e., via dative bonding) and is no longer available to perturb trans C−H modes.[3] The derivative-shaped ν(Si−H) mode at ∼2075 cm^{-1} in Figure 7a was noted previously and probably results from the shift of preexisting surface Si−H modes upon adsorption of *N*-methylpyrrolidine.[3] The total integrated intensity of the positive and negative portions of the derivative feature is slightly positive, which was attributed to a slight growth of Si−H modes from contamination sources (e.g., chamber hydrogen or water) concurrent with the experiments.

The IR spectrum of a saturation exposure (15 L) of *N*-methylpyrrolidine on the Ge(100)-2×1 surface, which has not been previously reported, is shown in Figure 7b. The spectrum is very similar to Figure 7a and thus indicates that *N*-methylpyrrolidine adsorbs through dative bonding on Ge(100) as well. Interestingly, by comparing the intensity of the C−H stretch region in Figure 6a and b, the coverage of *N*-methylpyrrolidine on Ge(100) appears to be significantly larger than on Si(100). We note that comparing the integrated intensities on Si(100) and Ge(100) to quantify relative coverages may be unreliable because the infrared transition dipole may differ on the two surfaces. However, in our experience, the relative intensities of infrared spectra for most organic molecules on Si(100) and Ge(100) are roughly equivalent on both surfaces.

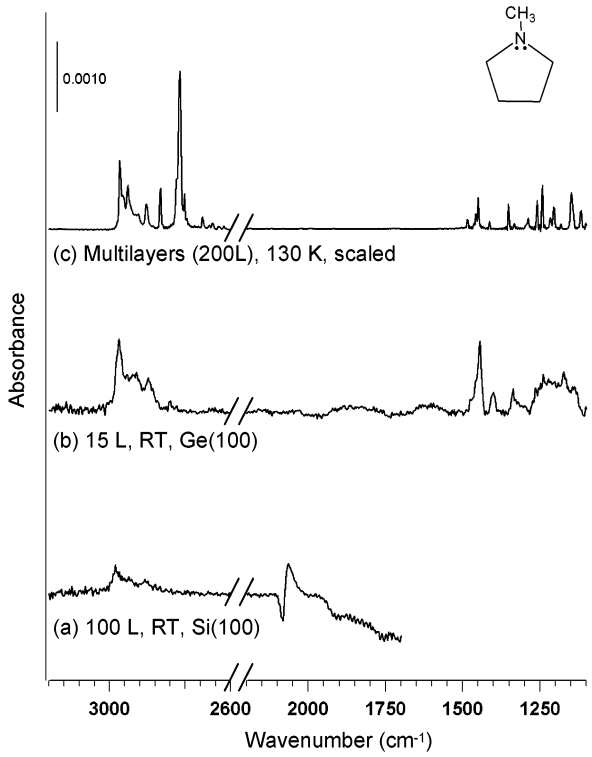

Figure 7. Infrared spectra of *N*-methylpyrrolidine on the Si(100)-2×1 and Ge(100)-2×1 surfaces: (a) 100 L at 298 K on Si(100). (b) 15 L at 298 K on Ge(100). (c) Multilayers (scaled) at 130 K.

We previously noted that the low saturation coverage of *N*-methylpyrrolidine on Si(100) compared to that of pyrrolidine may be due to steric effects that could destabilize the dative-bonded state.[3] For Ge(100), the slightly larger spacing between adjacent dimers in a row versus Si (4.00 Å versus 3.84 Å, respectively) may reduce steric repulsion between adjacent adducts and allow higher coverages to be stably attained. We also considered the possibility that destabilizing charge-transfer effects from dative-bonded adducts on adjacent dimers may play a role in the low saturation coverage of *N*-methylpyrrolidine. However, more recent and extensive calculations by Widjaja et al. showed that only the Si surface *atom* directly adjacent to the dative-bonded NH_3, not the entire adjacent dimer, needs to be unoccupied for the charge-transfer delocalization to occur.[38] From those results, it can be inferred that *N*-methylpyrrolidine can avoid destabilizing charge-transfer effects on Si(100) by adsorbing in the same alternating pattern down the dimer row. However, charge-transfer delocalization effects have not been examined on Ge(100), and it is possible that there may be differences from Si(100).

The calculated critical points on the potential energy surface for the N−CH_3 dissociation of *N*-methylpyrrolidine are shown in Figure 8. It is noted that dative bonding for *N*-methylpyrrolidine is ∼4 kcal/mol less favorable than for pyrrolidine on both Si(100) and Ge(100), most likely because of the steric effects from the *N*-methyl group.

Thus, to summarize the *N*-methylpyrrolidine results, *N*-methylpyrrolidine undergoes stable dative bonding at room temperature on both Si(100) and Ge(100) surfaces, with a significantly higher saturation coverage observed on the Ge(100) surface versus that on the Si(100) surface.

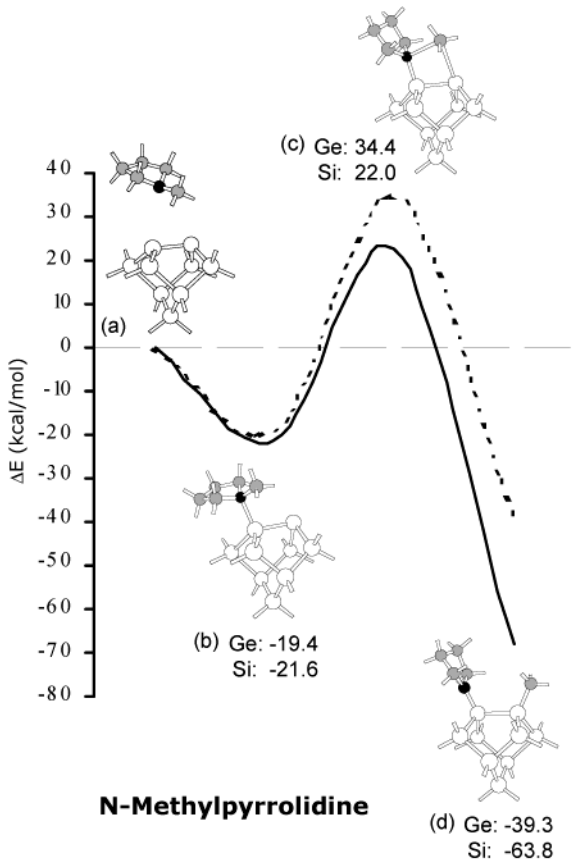

Figure 8. Critical points on the potential energy surfaces of the N−CH_3 dissociation reaction of *N*-methylpyrrolidine on Si(100)-2×1 and Ge(100)-2×1: (a) Reactants. (b) Dative-bonded precursor. (c) Transition state. (d) N−CH_3 dissociated product.

C. 3-Pyrroline. Studies of pyrrolidine and *N*-methylpyrrolidine provide information about the bonding of saturated amines with the Si(100) and Ge(100) surfaces. To probe the competition between the amino group and a C═C bond that may occur in an unsaturated amine, we have examined the chemistry of the unsaturated analogue of pyrrolidine, 3-pyrroline, on the Ge(100)-2×1 surface. The IR spectrum following a 5-L exposure of 3-pyrroline on Ge(100) at room temperature is shown in Figure 9a. A spectrum of unreacted 3-pyrroline multilayers at 110 K (scaled) is shown for comparison in Figure 9c. It is apparent in Figure 9a that no ν(Ge−H) mode appears, ruling out N−H dissociation of 3-pyrroline following the 5-L exposure. Additionally, the peak at 3090 cm^{-1}, which is assigned to an sp^2 ν(C−H) mode, has not decreased significantly in intensity relative to the ν(N−H) mode near 3250 cm^{-1} or the sp^3 ν(C−H) modes around 2850 cm^{-1} when compared to the multilayer spectrum. This indicates that there is no significant [2 + 2] cycloaddition product across the C═C bond of 3-pyrroline because this product would result in the loss of the sp^2 ν(C−H) mode. The spectrum is instead consistent with 3-pyrroline dative-bonded to the Ge(100) surface at a 5-L exposure. The attenuation of the Bohlmann band (at 2835 cm^{-1} in Figure 9c) upon adsorption indicates that the lone pair is involved in bonding and thus provides additional evidence for dative bonding.

Following an additional 25-L saturation exposure (30 L total) of 3-pyrroline on Ge(100), growth of all of the previous modes is seen, as well as a new peak at 1920 cm^{-1}. As with pyrrolidine, we assign this peak to a ν(Ge−H) mode that is substantially red-shifted (as was observed for pyrrolidine). Thus, like pyrrolidine, 3-pyrroline exhibits coverage-dependent adsorption behavior on Ge(100), with a fraction of the adsorbed species escaping the dative-bonded precursor state and undergoing N−H dissociation at higher coverages. Continued growth of the sp^2 ν(C−H) mode at 3084 cm^{-1} in Figure 9b indicates that no significant [2 + 2] C═C cycloaddition product is observed at higher coverage, although we cannot rule out its existence as a small side product.

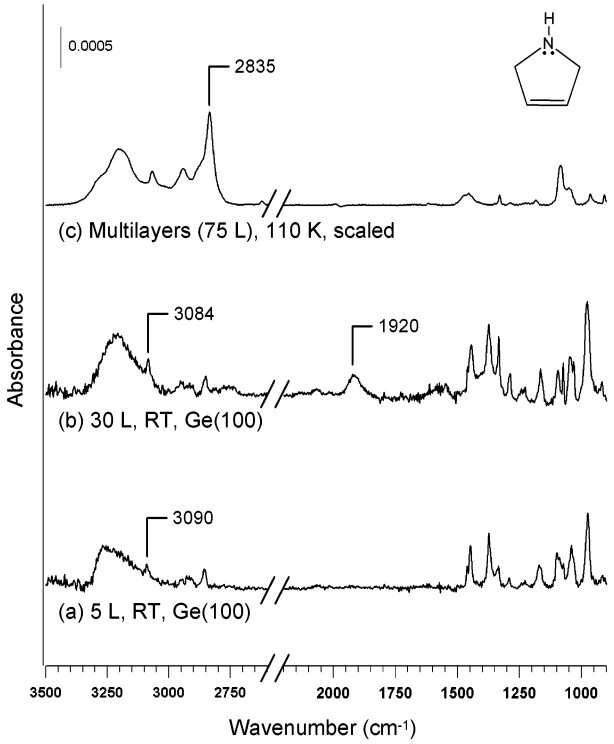

Figure 9. Infrared spectra of 3-pyrroline: (a) 5 L at 298 K on Si(100). (b) 30 L at 298 K on Ge(100). (c) Multilayers (scaled) at 110 K.

We have calculated the critical points on the potential energy surface for the N−H dissociation reaction of 3-pyrroline on the Si(100)-2×1 and Ge(100)-2×1 surfaces. The results are shown in Figure 10. It can be seen that the energetics for N−H dissociation of 3-pyrroline are nearly identical to those of pyrrolidine (Figure 6) on both Si(100) and Ge(100). Thus, the calculations indicate that the presence of the C═C bond in 3-pyrroline has a negligible effect on the energetics of the N−H dissociation reaction.

The adsorption energies of the [2 + 2] cycloaddition reaction on Si(100) and Ge(100) have also been calculated to be −38.4 and −23.4 kcal/mol, respectively. Although we could not locate transition states for the adsorption of 3-pyrroline on Si(100) and Ge(100) via [2 + 2] cycloaddition at the BLYP/6-31G(d) level of theory, Mui estimated the activation barriers for the adsorption of ethylene on Si(100) and Ge(100) via [2 + 2] cycloaddition to be 5.1 and 6.6 kcal/mol, respectively.[22] However, the formation of Si−N and Ge−N dative bonds has no activation barrier at all. Therefore, the calculations indicate that the [2 + 2] cycloaddition of 3-pyrroline is kinetically less favorable than dative bond formation.

We have not examined the reaction of 3-pyrroline on the Si(100)-2×1 surface. Cao et al. have previously studied this system using X-ray photoelectron spectroscopy (XPS) and MIR-FTIR spectroscopy[28] and reported a major N−H dissociation product. The absence of a significant ν(N−H) mode in their IR spectra indicated that no [2 + 2] cycloaddition or dative-bonded products were present on the surface. A second bonding

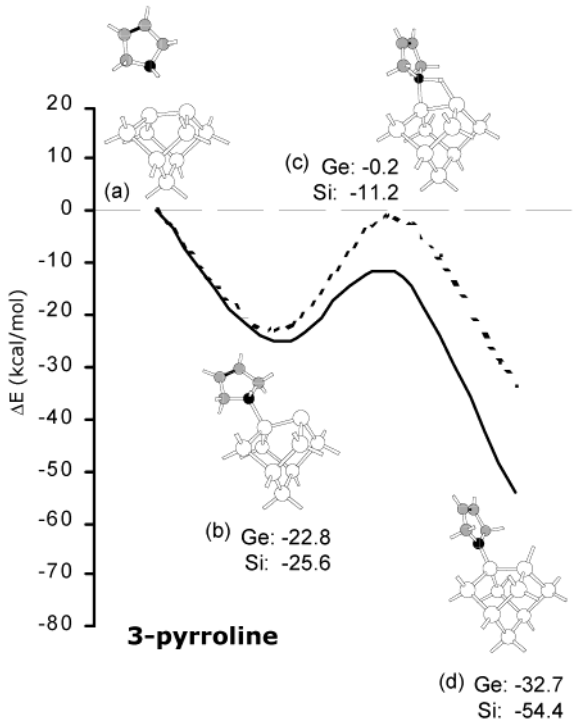

Figure 10. Critical points on the potential energy surfaces of the N−H dissociation reaction of 3-pyrroline on Si(100)-2×1 and Ge(100)-2×1: (a) Reactants. (b) Dative-bonded precursor. (c) Transition state. (d) N−H dissociated product.

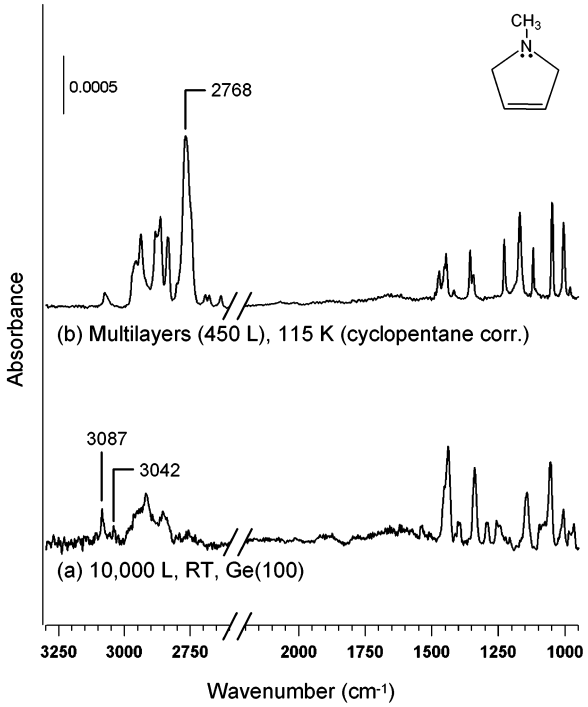

Figure 11. Infrared spectra of *N*-methyl-3-pyrroline on the Ge(100)-2×1 surface: (a) 10 000 L at 298 K on Ge(100). (b) Multilayers (scaled) at 115 K. The multilayer spectrum has been corrected for cyclopentane, which is the majority component in the *N*-methyl-3-pyrroline sample used, as described in the text.

configuration on Si(100)-2×1 indicated by XPS was assigned to a [2 + 2] cycloaddition product that had undergone dehydrogenation, although no mechanism for the dehydrogenation step was proposed.[28]

To summarize, 3-pyrroline primarily undergoes dative bonding on the Ge(100) surface at room temperature, with N−H dissociation also occurring at higher coverages. The IR results and the DFT calculations suggest that [2 + 2] cycloaddition does not compete to a significant degree.

D. *N*-Methyl-3-pyrroline. The reaction of *N*-methyl-3-pyrroline on Ge(100)-2×1 was also examined to determine whether a methyl-protecting group would hinder reaction at the nitrogen and allow the [2 + 2] cycloaddition reaction to occur. The IR spectrum of the Ge(100) surface following a saturation exposure (10 000 L) to *N*-methyl-3-pyrroline (in a 5:1 cyclopentane/*N*-methyl-3-pyrroline solution) at room temperature is shown in Figure 11a. The large exposure necessary to attain saturation is attributed to the higher volatility of cyclopentane, which is thus dosed in a much larger (though undetermined) proportion relative to *N*-methyl-3-pyrroline. An independent experiment was carried out to verify that cyclopentane does not react with the Ge(100) surface. Similar to the spectrum of *N*-methylpyrrolidine (Figure 7c), the physisorbed multilayer spectrum (115 K) of *N*-methyl-3-pyrroline (Figure 11b) exhibits a strong Bohlmann band at 2768 cm^{-1} due to the interaction of the N lone pair with trans-periplanar C−H bonds. This mode is greatly reduced in intensity following the adsorption of *N*-methyl-3-pyrroline onto Ge(100) (Figure 11a), indicating dative bonding to the surface. Peaks at 3042 and 3087 cm^{-1} in Figure 11a are assigned to sp^2 ν(C−H) modes. The strong intensity of the sp^2 ν(C−H) 3087-cm^{-1} peak relative to the sp^3 ν(C−H) modes, when compared to the multilayer spectrum (Figure 11b), suggests little or no [2 + 2] cycloaddition of *N*-methyl-3-pyrroline because this reaction requires the consumption of the C═C bond. Thus, despite the absence of an N−H dissociation pathway, the [2 + 2] cycloaddition reaction still does not compete significantly with dative bonding.

Although we have not performed calculations for *N*-methyl-3-pyrroline, the energetics for N−CH_3 dissociation are expected to be very similar to those calculated for *N*-methylpyrrolidine (Figure 8) on the basis of the comparison of the calculations for 3-pyrroline and pyrrolidine. Hence, as with *N*-methylpyrrolidine, N−CH_3 dissociation is also unlikely for *N*-methyl-3-pyrroline on Si(100)-2×1 and Ge(100)-2×1 because of a prohibitive barrier at room temperature.

The kinetic competition between [2 + 2] cycloaddition and dative bond formation has already been discussed in the previous section regarding 3-pyrroline, and the surface reaction energetics of *N*-methyl-3-pyrroline are expected to be similar. Therefore, *N*-methyl-3-pyrroline adsorbs on the Ge(100) surface via dative bonding at room temperature, and [2+2] cycloaddition adducts are not formed in significant concentrations.

E. Pyrrole. (i) IR Results for Pyrrole Adsorption. An IR spectrum of the Ge(100) surface following a saturation dose (100 L) of pyrrole at room temperature is shown in Figure 12b. The physisorbed spectrum of pyrrole multilayers at 110 K (scaled) is shown for comparison in Figure 12d. A significant peak at 1988 cm^{-1} in Figure 12b indicates that Ge−H bonds are present at the surface following chemisorption. In contrast to the large red shift observed for the ν(Ge−H) modes of pyrrolidine and 3-pyrroline on Ge(100), the absence of a red shift of the ν(Ge−H) mode for pyrrole suggests that dative-bonded species are not present in a significant amount. Coupled with the large loss in intensity of the ν(N−H) mode compared with the physisorbed spectrum (scaled), the presence of the ν(Ge−H) mode indicates that the majority of pyrrole undergoes N−H dissociation upon adsorption onto the Ge(100) surface. However, the retention of a small ν(N−H) mode at 3403 cm^{-1} indicates that some pyrrole reacts through other pathways that do not break the N−H bond.

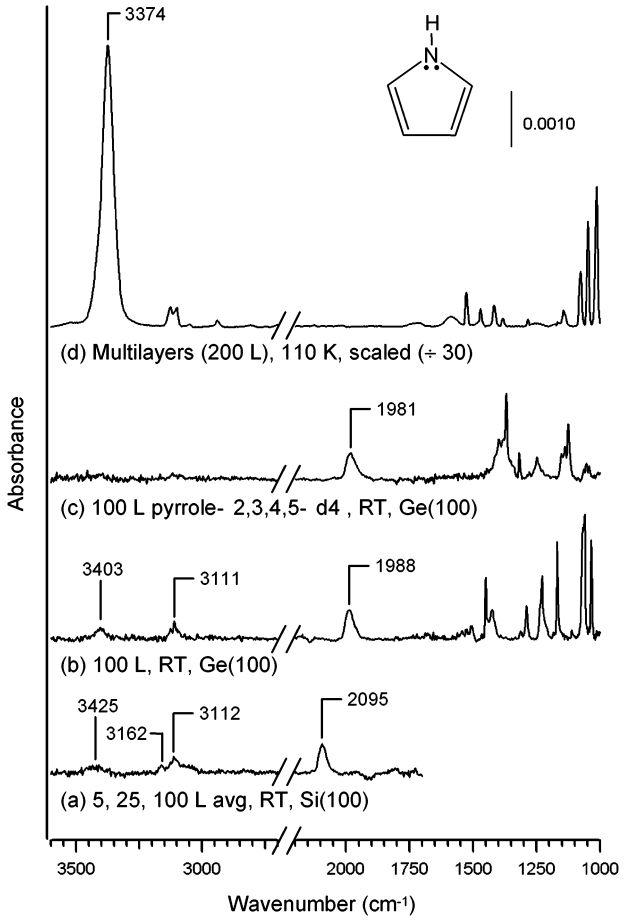

Figure 12. Infrared spectra of pyrrole on the Si(100)-2×1 and Ge(100)-2×1 surfaces: (a) Saturation dose (average of 5-, 25-, and 100-L doses) at 298 K on Si(100). (b) 100 L at 298 K on Ge(100). (c) 100 L of pyrrole-2,3,4,5-d_4 on Ge(100) at 298 K. (d) Multilayers (scaled) at 110 K.

Out of the other possible reaction pathways considered for pyrrole, shown in Figure 2, the [2 + 2] and [4 + 2] cycloaddition reactions would retain the N−H bond and result in both sp^3-hybridized ν(C−H) and nonaromatic sp^2-hybridized ν(C−H) modes. However, it is apparent that no significant sp^3 ν(C−H) modes, which would occur in the 2800−3000 cm^{-1} region of the spectrum and are typically stronger in intensity than sp^2 ν(C−H) modes, are present in Figure 12b. Nor can significant peaks be seen in the 3000−3100 cm^{-1} region, which are indicative of nonaromatic sp^2 ν(C−H) modes in cyclic amines. The only major ν(C−H) mode in the spectrum, at 3111 cm^{-1}, arises from aromatic groups. Thus, the IR data indicate that the [2 + 2] and [4 + 2] cycloaddition reactions of pyrrole are not competitive with N−H cleavage on Ge(100) at room temperature.

Another possible reaction that can account for the ν(N−H) mode in Figure 12b is the attachment of pyrrole to the surface via a ring carbon and the transfer of a ring hydrogen to the surface, as shown in Figure 2f. This C−H dissociation surface reaction is analogous to electrophilic aromatic substitution (EAS) in organic chemistry. We have performed isotopic labeling studies to determine whether pyrrole undergoes EAS at the Ge(100) surface. Figure 12c shows the IR spectrum of the Ge(100) surface following a saturation exposure (100 L) to pyrrole-2,3,4,5-d_4 in which all of the hydrogens attached to ring carbons have been replaced with deuterium. Interestingly, a ν(N−H) mode is not observed above the noise level in Figure 12c. This result is surprising because the normal compound did exhibit an N−H stretch in the spectrum (Figure 12b) and hence did not react completely by N−H cleavage, whereas the isotopic substitution results on the deuterated compound suggest that virtually all of pyrrole-2,3,4,5-d_4 has reacted by N−H dissociation. Thus, it appears that the side reaction leading to the remaining ν(N−H) mode for normal pyrrole has been suppressed for pyrrole-2,3,4,5-d_4. This suppression for the deuterated isotope can be explained by a kinetic isotope effect in which the substitution of hydrogen with deuterium leads to a retardation of the rate for a C−H/D dissociation (i.e., EAS) reaction. The data are thus consistent with the assignment of electrophilic aromatic substitution as the side reaction that is evidenced by the remaining ν(N−H) peak for normal pyrrole on Ge(100).

TABLE 1: Theoretical Results for Pyrrole and *N*-Methylpyrrole[a]

	pyrrole		*N*-methylpyrrole	
	Si	Ge	Si	Ge
N-dative	−0.6	−1.6		
N−H/N−CH_3 dis. t.s.	6.4	13.3	32.4	
N−H/N−CH_3 dis.	−52.6	−34.3	−64.4	−43.1
[2 + 2] cycloaddition t.s.	2.2	7.7	1.9	7.7
[2 + 2] cycloaddition	−13	0.0	−13.6	−0.4
[4 + 2] cycloaddition	−21.0	−7.6	−20.1	−7.8
α-C dative	−6.6	−7.4	−7.3	
α-C−H dis. t.s. (direct)	7.1	14.2	7.0	
α-C−H dis. (EAS)	−47.6	−32.2	−46.7	−31
β-C dative	−4.1	−6.2	−5.8	
β-C−H dis. t.s. (direct)	11.2	17.8	9.4	
β-C−H dis. (EAS)	−47.6	−32.2	−47.9	
N−H dis. t.s. from α-C dative	−2.7	3.4	NA	NA
N−H dis. from α-C dative	−32.5	−19.7	NA	NA
α-C to N surface transfer	−21.0	−8.1	NA	NA
α-C to N−H transfer t.s.	−1.8	13.1	NA	NA
CH_2−H dis. t.s.	NA	NA	34.5	
CH_2−H dis.	NA	NA	−42.4	−29.4

[a] Units are kcal/mol; NA = not applicable.

The IR spectrum of a saturation exposure of pyrrole on the Si(100) surface is shown in Figure 12a. The spectrum is very similar to that of pyrrole on Ge(100), with a ν(Si−H) peak at 2095 cm^{-1}, aromatic sp^2 ν(C−H) modes at 3112 and 3162 cm^{-1}, and a small, residual ν(N−H) peak at ∼3430 cm^{-1}. These results indicate that N−H dissociation is the major but not the only reaction on Si(100). Earlier studies have also reported that the major product for pyrrole on Si(100)-2×1 is formed by N−H dissociation.[15,28] In one of these previous studies by Cao et al., some remaining intensity in the IR spectrum was also observed in the ν(N−H) mode; this result was attributed to a side reaction involving both the N−H and C−H cleavage of pyrrole, although no mechanism for this reaction was proposed.[28] Although we have not performed isotopic labeling studies of pyrrole on Si(100), we believe that electrophilic aromatic substitution can account for the remaining ν(N−H) mode on the Si(100) surface.

(ii) Theoretical Results for Pyrrole Adsorption. We have performed theoretical calculations to examine the N−H dissociation and electrophilic aromatic substitution reaction pathways for pyrrole on both the Si(100)-2×1 and Ge(100)-2×1 surfaces. The results, along with calculated energetics for the [2 + 2] and [4 + 2] cycloaddition reactions, are shown in Table 1. We begin our discussion of the theoretical results with N−H dissociation, which was found experimentally to be the major reaction pathway on both surfaces. Figure 13a shows the calculated critical points on the potential energy surface for the direct N−H dissociation pathway for pyrrole, which proceeds, analogously to that of pyrrolidine and 3-pyrroline, through a nitrogen dative-bonded precursor state. What is most different from pyrrolidine and 3-pyrroline in these results are the weak

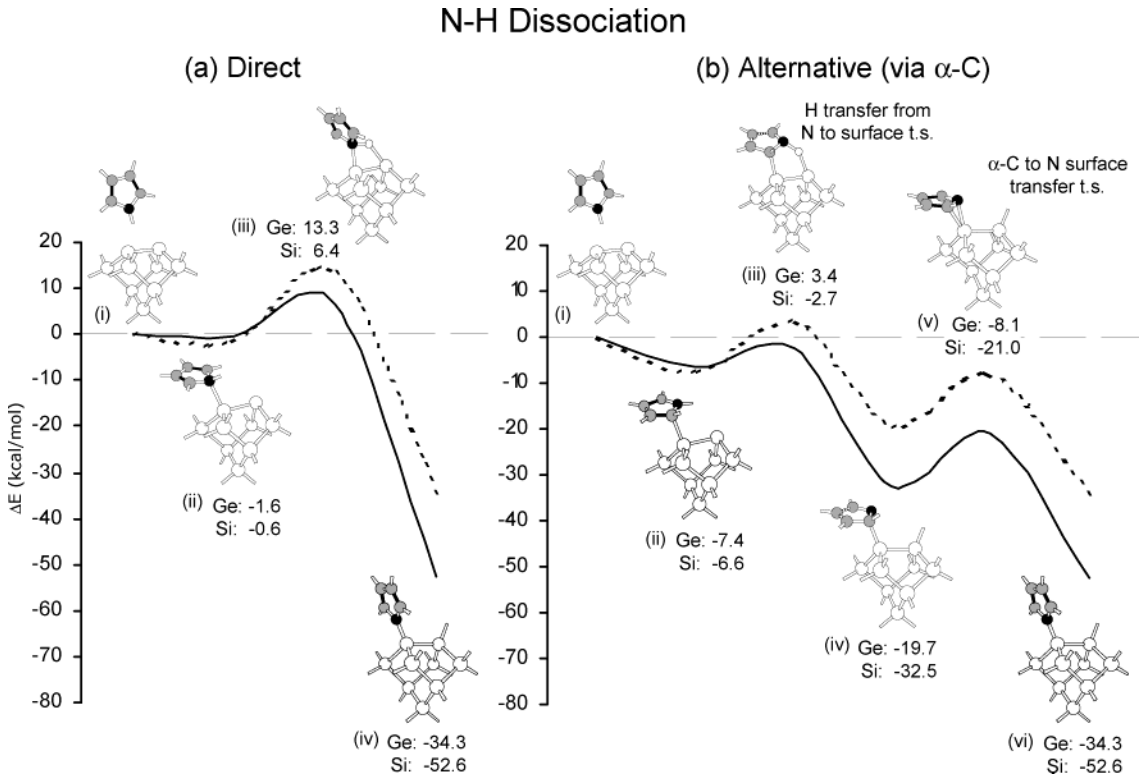

Figure 13. Critical points on the potential energy surfaces of the N−H dissociation reaction of pyrrole on Si(100)-2×1 and Ge(100)-2×1: (a) Direct pathway. (b) Alternative pathway (shown through the α-C).

energies of the nitrogen dative-bonded states for pyrrole. At −0.6 and −1.6 kcal/mol on the Si(100) and Ge(100) surfaces, respectively, the binding energies of the dative-bonded state are approximately 21 to 25 kcal/mol less stable than those calculated for pyrrolidine and 3-pyrroline. This result is expected because of the description of pyrrole as an aromatic compound in which the "lone pair" is delocalized over the ring and comprises part of the aromatic π system. The weaker adsorption energies of nitrogen dative-bonded pyrrole are thus attributed to the loss in resonance energy that accompanies dative bonding. This thermodynamic penalty for pyrrole to form a dative bond is roughly consistent with the estimated resonance energy of ∼24 kcal/mol.[39]

Because of the loss in aromaticity, the transition-state energies relative to the energy of the reactants for N−H dissociation from the nitrogen dative-bonded precursor states are also significantly higher than those for the aliphatic amines, pyrrolidine and 3-pyrroline. Whereas for pyrrolidine and 3-pyrroline the barriers for direct N−H dissociation are calculated to lie below the energy of the reactants, for pyrrole the barriers for direct N−H dissociation are 6.4 and 13.3 kcal/mol above the energy of the reactants for Si(100) and Ge(100), respectively, as seen in Figure 13a. However, the experimental measurements show that N−H dissociation occurs readily for pyrrole on both Si(100) and Ge(100) despite barriers that very few molecules are expected to surmount at room temperature. The experimental results therefore suggest that an alternative, lower-energy N−H dissociation pathway may exist.

We have calculated a more kinetically favorable pathway leading to N−H dissociation of pyrrole on both Si(100) and Ge(100). An analogous pathway has been independently calculated by Luo et al. on the Si(100)-2×1 surface only.[18] This pathway, shown in Figure 13b, proceeds via initial attachment at the α-C rather than at the nitrogen and involves an additional transition state. Molecular adsorption at a carbon atom, analogous to dative bonding at the nitrogen, is facilitated in pyrrole because of its delocalized system of π electrons. In aliphatic amines such as pyrrolidine and 3-pyrroline, such a carbon dative-bonded state would be highly unstable because this would result in a pentavalent carbon. Interestingly, for pyrrole, dative bonding through an α-C, shown in Figure 13b(ii), is actually more energetically favorable than dative bonding through the nitrogen, even though dative bonding at both positions requires breaking aromaticity. From the α-C dative-bonded state, pyrrole can transfer the hydrogen from nitrogen directly to the surface to form the nonaromatic, metastable state shown in Figure 13b-(iv). As can be seen in Figure 13, the barrier for this step is lower in energy than the barrier for direct N−H dissociation (Figure 13a) from the nitrogen dative-bonded precursor state. From the metastable structure in Figure 13b(iv), there is less than a 12 kcal/mol barrier that is below the energy of the reactants for the N atom and α-C to exchange positions on both surfaces, resulting in the final N−H dissociated state in Figure 12a(iv) and b(vi). This step is calculated to be rapid at room temperature versus the reverse step leading back to the dative-bonded state shown in Figure 13b(ii).

For the direct pathway shown in Figure 13a, N−H dissociation must compete unfavorably with the negligible barrier for reversible desorption from the nitrogen dative-bonded precursor state back to the vacuum. Additionally, the direct pathway is calculated to have barriers several kcal/mol above the energy of the reactants on both surfaces. The alternative pathway (Figure 13b) is calculated to be kinetically favorable to the direct pathway because it is unactivated on Si(100) and only slightly above the energy of the reactants at one transition state on Ge(100). Thus, the calculations suggest that pyrrole undergoes N−H dissociation via the alternative pathway rather than via the direct pathway through nitrogen.

We have calculated two EAS reaction pathways leading to the attachment of pyrrole at one of its ring carbons on both

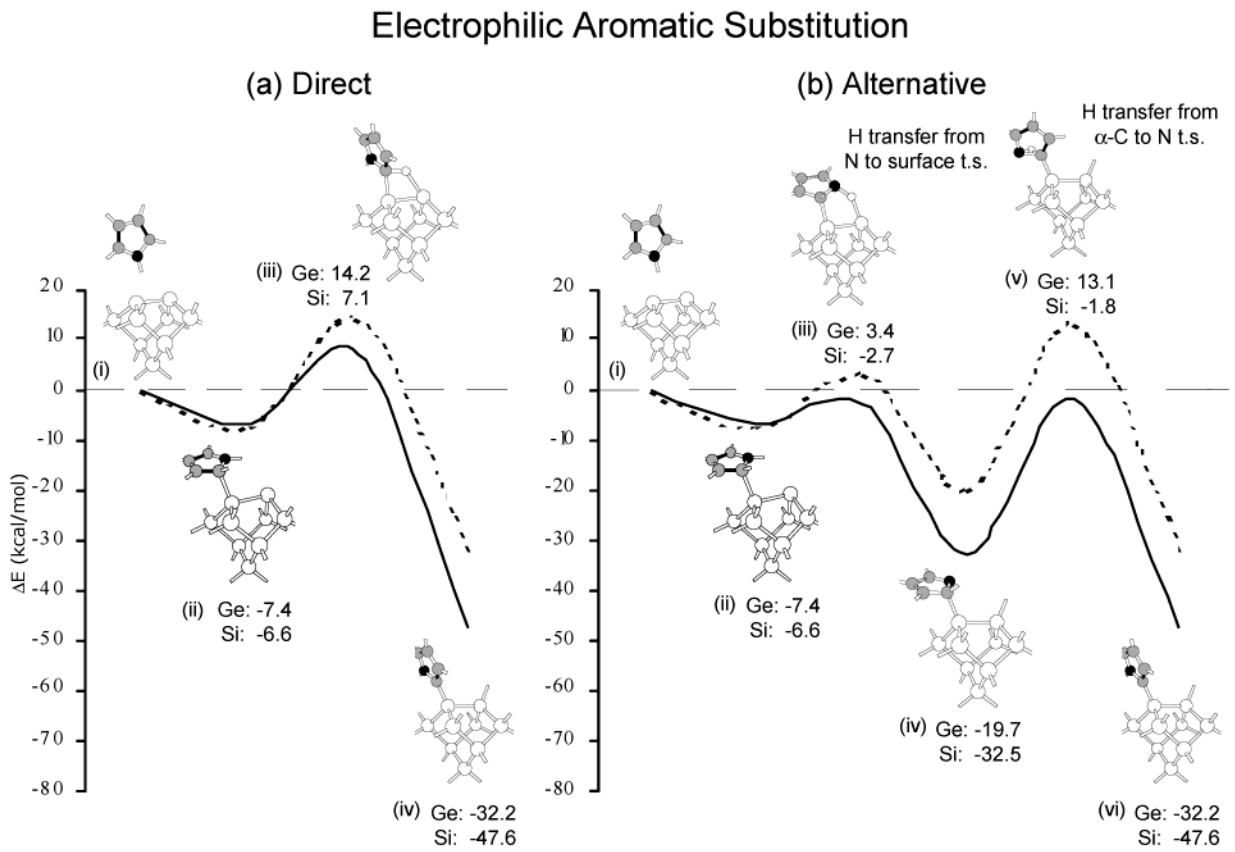

Figure 14. Critical points on the potential energy surfaces of the electrophilic aromatic substitution reaction of pyrrole on Si(100)-2×1 and Ge(100)-2×1: (a) Direct pathway. (b) Alternative pathway involving initial H loss from the nitrogen atom followed by hydrogen transfer from the α-C to the nitrogen atom.

Si(100) and Ge(100), which are shown in Figure 14. Both pathways occur through the same α-C dative-bonded precursor state as the alternative N−H dissociation pathway. The direct pathway for EAS, shown in Figure 14a, is the C−H dissociation analogue to the direct pathway for N−H dissociation (Figure 13a), with dative bonding and hydrogen transfer occurring at the same C atom. The energetics of the direct EAS and N−H dissociation pathways are also very similar, with the exception of the dative-bonded state, which is more stable through C than through N. We have calculated the EAS pathway at the β-C as well (on Si only) and have found that the barrier is ∼4 kcal/mol higher in energy than at the α-C.

The calculated alternative pathway for EAS is shown in Figure 14b. The first part of this pathway is identical to the alternative N−H dissociation pathway, with initial attachment at the α-C and transfer of the hydrogen on the nitrogen to the surface. This is followed by transfer of the hydrogen from the dative-bonded α-C to the nitrogen (Figure 14b(v)), resulting in the EAS product in Figure 14b(vi), which restores aromaticity to the molecule. Whereas this pathway is unactivated on the Si(100) surface, it has a substantial barrier of 30.7 kcal/mol from the metastable state (Figure 14b(iv)) and must compete against N−H dissociation (Figure 13b), which has a smaller 11.5 kcal/mol barrier from the same state. On Ge(100), the alternative pathway for EAS in Figure 14b appears to be even less favorable than the direct pathway, with a second transition state (Figure 14b(v)) 33.4 kcal/mol above the metastable state (Figure 14b-(iv)) and 13.3 kcal/mol above the energy of the reactants. The calculated barriers of both EAS pathways on Ge(100) for pyrrole seem too large to explain the observation of the reaction at room temperature. It is possible that a lower-energy pathway that we have not yet located exists for the EAS reaction. The calculation that the EAS reaction of pyrrole has a larger barrier than the N−H dissociation reaction is, however, consistent with the experimental observation that it is produced in lower yield. In addition, defects may play a role in the relative branching ratios of these two reactions, especially if defects exhibit electrophilic characteristics.

In summary, the IR results and theoretical calculations indicate that pyrrole undergoes N−H dissociation on both the Si(100) and Ge(100) surfaces at room temperature, leading to the formation of covalent surface Si−N or Ge−N bonds as well as Si−H or Ge−H bonds, respectively. N−H dissociation is predicted to occur through an alternative pathway involving dative bonding at a ring carbon rather than at the nitrogen, which is made possible by the aromaticity of pyrrole. Evidence for a minor electrophilic aromatic substitution product resulting from C−H cleavage is also observed on both surfaces. Both N−H dissociation and electrophilic aromatic substitution products result in the retention of aromaticity.

F. *N*-Methylpyrrole. As the methyl-capped analogue of pyrrole, *N*-methylpyrrole can undergo all of the same reactions as pyrrole with the Si(100) and Ge(100) surfaces except that the N−H dissociation reaction is replaced by an N−CH_3 dissociation reaction, as shown in Figure 2. Additionally, *N*-methylpyrrole may undergo chemisorption through the cleavage of a C−H bond from its methyl group, as shown in Figure 15. Coulter et al. previously reported that the methyl-substituted aromatic compounds toluene and xylene undergo some C−H dissociation from their methyl groups rather than from the aromatic ring upon adsorption onto Si(100).[40]

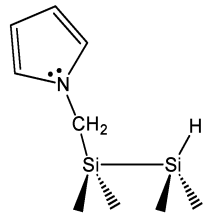

Ge: -29.4 kcal/mol
Si: -42.4 kcal/mol

CH_2-H Dissociation

Figure 15. Calculated CH_2-H dissociation product of *N*-methylpyrrole on Si(100)-2×1 and Ge(100)-2×1 (shown for Si).

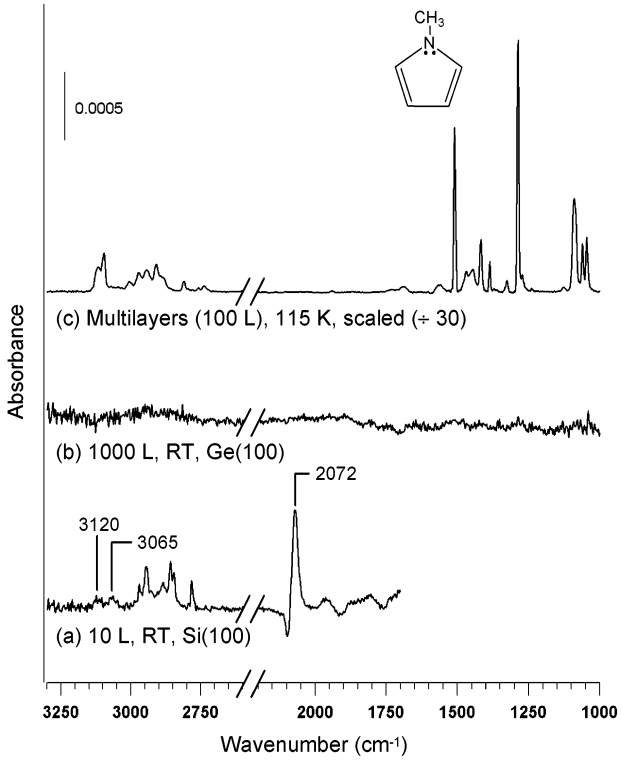

Figure 16. Infrared spectra of *N*-methylpyrrole on the Si(100)-2×1 and Ge(100)-2×1 surfaces: (a) 10 L (average of three spectra) at 298 K on Si(100). (b) 1000 L at 298 K on Ge(100). (c) Multilayers (scaled by $^1/_{30}$) at 115 K.

The IR spectra of the Ge(100) and Si(100) surfaces following exposure to *N*-methylpyrrole at room temperature are shown in Figure 16. Interestingly, no significant reaction is observed on Ge(100) following 1000-L (Figure 16b) or higher exposures to *N*-methylpyrrole, whereas on Si(100) saturation is reached at an exposure of 10 L (Figure 16a). Peaks at 3120 and 3065 cm^{-1} in the Si spectrum are assigned to aromatic and nonaromatic sp^2-hybridized ν(C−H) modes, respectively. This assignment indicates products in which aromaticity has been retained (e.g., EAS) and products in which aromaticity has been broken on the surface (e.g., [4 + 2] cycloaddition). The presence of a ν(Si−H) peak at 2072 cm^{-1} in Figure 16a further indicates that some of the adsorption occurs via C−H cleavage either through EAS or methyl C−H dissociation.

An examination of the theoretical results, shown in Table 1, is helpful in narrowing down the possible surface products on Si(100). We consider first the three possible reactions that result in the retention of aromaticity in the product. These are the $N-CH_3$ dissociation reaction (Figure 2c), the methyl C−H dissociation reaction (Figure 15), and the EAS reaction (Figure 2f). The energetics for EAS of *N*-methylpyrrole are very similar to those calculated for pyrrole, with substitution at the β-C being slightly less kinetically favorable than at the α-C. The barriers for both the $N-CH_3$ dissociation reaction and the methyl C−H dissociation reaction are both prohibitively high, lying 32.4 and 34.5 kcal/mol above the energy of the reactants, respectively. Thus, the theoretical results suggest that the aromatic product on the Si(100) surface is the result of an EAS reaction.

To account for the presence of the nonaromatic sp^2 ν(C−H) mode on the surface, we have examined theoretically the possibility of [2 + 2] and [4 + 2] cycloaddition reactions of *N*-methylpyrrole. For the [2 + 2] cycloaddition reaction of *N*-methylpyrrole on Si(100), we calculate only a minor barrier. For the [4 + 2] cycloaddition reaction, we were unable to locate a transition state, suggesting that a barrier may not exist or that the potential energy surface for this reaction is very flat. Both [2 + 2] and [4 + 2] cycloaddition reactions are known to be facile on the Si(100) surface and have been observed experimentally in previous studies of other molecules.[41−45] However, because of the loss of aromaticity suffered, the binding energies of the cycloaddition products of pyrrole and *N*-methylpyrrole are substantially weaker than those of nonaromatic unsaturated compounds (e.g., 3-pyrroline). In fact, with a calculated desorption energy ΔE_{des} of only 15 kcal/mol, the [2 + 2] cycloaddition product has a mean surface lifetime of only ∼0.01 s at room temperature, using a first-order Arrhenius expression and a preexponential factor of 10^{13} s^{-1}. Dative-bonded *N*-methylpyrrole through either the C atom or the N atom is also nonaromatic and is predicted (based on the pyrrole calculations) to be even less stable than the [2 + 2] cycloaddition product on both Si(100) and Ge(100). Thus, in addition to undergoing an EAS reaction, *N*-methylpyrrole reacts most likely via a [4 + 2] cycloaddition reaction on the Si(100) surface at room temperature.

In summary, the IR results and theoretical calculations suggest that *N*-methylpyrrole undergoes both electrophilic aromatic substitution and [4 + 2] cycloaddition reactions on the Si(100) surface at room temperature. On the Ge(100) surface, no stable products are observed at room temperature.

IV. Discussion

A. Reactivity of Aliphatic Amines. An examination and comparison of the reactions of a series of increasingly functional cyclic amines, both aliphatic and aromatic, on Si(100)-2×1 and Ge(100)-2×1 offers valuable insight into the reactivity of clean semiconductor surfaces. We begin our discussion with the aliphatic amines in this study: pyrrolidine, *N*-methylpyrroline, 3-pyrroline, and *N*-methyl-3-pyrroline.

The reactivity of all of the aliphatic amines is determined in large part by their ability to form strong dative bonds to the surface via the nitrogen lone pair. Whereas the dative-bonded state can be considered to be a metastable precursor to N−H dissociation and $N-CH_3$ dissociation, it has a sufficiently large binding energy at room temperature to compete as an observable reaction product. On the Si(100) surface, the barrier for N−H dissociation of pyrrolidine and 3-pyrroline is low enough that no dative-bonded adducts are observed at room temperature. However, on Ge(100), the larger barrier for N−H dissociation results in a trapping of the majority of adsorbed pyrrolidine and 3-pyrroline molecules in the dative-bonded precursor state. For the tertiary amines *N*-methylpyrrolidine (examined on Si(100) and Ge(100)) and *N*-methyl-3-pyrroline (examined on Ge(100)), only dative-bonded surface species are observed because of the prohibitive barrier for $N-CH_3$ dissociation.

Whereas the IR results indicate that the initial adsorption of pyrrolidine and 3-pyrroline on Ge(100) results in stably bound dative-bonded species, at higher coverages some N−H dissociation does occur. This is of interest, especially because another simple secondary amine, dimethylamine, was not observed to undergo N−H dissociation on Ge(100)-2×1 even at saturation coverages.[6] The difference in adsorption behavior between pyrrolidine and 3-pyrroline versus dimethylamine on Ge(100) suggests that the barrier for N−H dissociation may be lower for pyrrolidine and 3-pyrroline. Using a full nine-atom one-dimer Ge(100)-2×1 cluster for consistency with previous dimethylamine calculations and employing the same level of theory, we have calculated that the transition-state energy for pyrrolidine on Ge(100)-2×1 is 1.9 kcal/mol below the energy of the reactants, compared to 0.1 kcal/mol *above* the energy of the reactants for dimethylamine. Thus, the calculations do predict a slightly lower barrier for N−H dissociation for pyrrolidine than for dimethylamine. Although the difference is small, it may explain why some N−H dissociation is observed for pyrrolidine and not for dimethylamine. It may also be possible that the explanation lies in coverage effects which make N−H dissociation accessible to pyrrolidine and 3-pyrroline on Ge(100) but do not exist or are kinetically less favorable for dimethylamine at high coverages. Adsorption at or near defect sites on the surface probably cannot explain the difference in reactivity because the sample preparation and chamber that was used were the same for the dimethylamine experiments and the experiments performed in the current study.

Our calculations indicate that the energetics of N−H dissociation for 3-pyrroline are nearly identical to those for pyrrolidine on both Si(100) and Ge(100). Hence, it is seen that the presence of the C═C bond in 3-pyrroline, which allows for the possibility of a [2 + 2] cycloaddition reaction, has no significant effect on the energetics of dative bonding or the N−H dissociation reaction. With no evidence for significant [2 + 2] cycloaddition products for 3-pyrroline and *N*-methyl-3-pyrroline on Ge(100), it also appears that the [2 + 2] cycloaddition reaction does not compete favorably with dative bonding or, in the case of higher coverages, N−H dissociation. Consequently, whereas the methyl groups on *N*-methylpyrrolidine and *N*-methyl-3-pyrroline remove the possibility of dissociation reactions at the nitrogen and hence act as a protecting group against N−H cleavage, they do not sufficiently hinder dative bonding to make it unstable at room temperature, nor do they create a barrier to dative bonding. Thus, *N*-methyl groups do not appear to be a good choice of "protecting group" for aliphatic amines if a reaction (e.g., [2 + 2] cycloaddition) at another site of the molecule is desired with the surface because dative bonding is likely to occur even if dissociation reactions do not.

The rates of reversible desorption (using a first-order Arrhenius expression and a preexponential factor of 10^{13} s^{-1}) for all of the competing reaction products of the aliphatic amines are negligible at room temperature, eliminating the possibility for equilibrium, or thermodynamic, control. Thus, the reactions of aliphatic amines on Si(100) and Ge(100) can be understood by classifying them as being under kinetic control, which the final product distribution will reflect. The calculations of Mui indicated that the reaction of the C═C functionality on Si(100) and Ge(100) via [2 + 2] cycloaddition has an overall activation barrier of a few kcal/mol.[22] In contrast, dative bonding of aliphatic compounds to the down, electrophilic atom of the Si(100)-2×1 and Ge(100)-2×1 dimers is calculated to be a barrierless process and hence proceeds over [2 + 2] cycloaddition. From the dative-bonded precursor state, the molecule can proceed to undergo a dissociation reaction at the nitrogen if the barrier is kinetically accessible. If the barrier is not accessible, then the observed product at room temperature will be the metastable dative-bonded precursor. This description can account for the observed reactivity of the aliphatic amines on the Si(100) and Ge(100) surfaces.

B. Reactivity of Aromatic Amines. The presence of conjugated double bonds and a lone pair in pyrrole and *N*-methylpyrrole results in a delocalization of π electrons that imparts aromaticity to the molecules. In this section, we discuss how this aromaticity defines the reactivity of pyrrole and *N*-methylpyrrole, resulting in substantially different chemistry on Si(100) and Ge(100) than that observed for aliphatic amines.

One significant consequence of aromaticity is that the delocalized ring of six π electrons in pyrrole and *N*-methylpyrrole permits dative bonding to occur via donation of two π electrons at all positions of the ring, including the α and β carbons, rather than just at the nitrogen. This ability allows alternative reaction pathways to be accessed that may be kinetically favorable, such as the alternative N−H dissociation pathway for pyrrole discussed in the Results section (Figure 13). The existence of the alternative N−H dissociation pathway is supported by the IR experiments that indicate that N−H dissociation is more facile on Ge(100) for pyrrole than for dimethylamine,[6] pyrrolidine, and 3-pyrroline, which are nonaromatic and hence have only the direct pathway through the nitrogen available to them. On the Ge(100)-2×1 surface at room temperature, pyrrole undergoes N−H dissociation at all coverages, whereas pyrrolidine and 3-pyrroline undergo N−H dissociation only at high coverages and dimethylamine does not undergo any significant N−H dissociation.[6]

Whereas the experiments on Ge suggest that the alternative N−H dissociation pathway for pyrrole may be favored over the direct dissociation pathways for aliphatic amines, it is actually calculated to have a transition state (3.4 kcal/mol) higher in energy relative to the reactants than that for the direct pathway for pyrrolidine (−1.0 kcal/mol) and 3-pyrroline (−0.2 kcal/mol) on Ge(100). This is the likely result of the substantially weaker dative-bonded precursor state for pyrrole, which increases the energy of its transition-state energy relative to that of pyrrolidine and 3-pyrrolidine. However, we calculate that the barrier from the dative-bonded precursor state to the first transition state for the alternative pathway of pyrrole (ΔE_{act} = 10.8 kcal/mol, Figure 13b) is substantially less than that for the direct pathway for pyrrolidine (ΔE_{act} = 21.9 kcal/mol, Figure 6) and 3-pyrroline (ΔE_{act} = 22.6 kcal/mol, Figure 10) on Ge(100). That is, despite the higher transition-state energy that must be passed through relative to the reactants, pyrrole can traverse through a more shallow potential energy well in comparison to pyrrolidine and 3-pyrroline to undergo N−H dissociation. The depth of the potential well is an important factor even for unactivated pathways because accommodation may occur in the dative-bonded precursor state, as seen previously for acetone on Ge(100).[5] This explanation may account for why N−H dissociation is more facile for pyrrole on Ge than for aliphatic amines such as pyrrolidine, 3-pyrroline, and dimethylamine.

Another significant effect of aromaticity is that reaction products that experience a loss of aromaticity will have weakened binding energies (and hence lower barriers to desorption) because of a loss of resonance energy. In many cases, this destabilization may be sufficient to cause the reversible desorption of the product, allowing more thermodynamically favorable reaction products to form, even if their formation is

TABLE 2: Comparison of Molecular and Surface Reactivity of Pyrrole

molecular reactivity	reactivity on semiconductor surfaces
pyrrole less basic than aliphatic amines	dative bonding less favorable for pyrrole than for aliphatic amines
thermodynamic preference for protonation is α-C > β-C > N	thermodynamic preference for dative bonding is α-C > β-C > N
pyrrole more acidic than aliphatic amines	N−H dissociation more facile on Ge for pyrrole than for aliphatic amines
pyrrole more reactive than benzene toward electrophilic substitution reactions	electrophilic substitution observed for pyrrole on Si and Ge but not for benzene or derivatives
proton transfer is 10−100 times faster at N than at ring carbons	N−H dissociation is faster than electrophilic substitution at ring carbons

less kinetically favorable (but still accessible). Because of this destabilization, dative-bonded pyrrole and *N*-methylpyrrole are not observed at room temperature on either Si(100) or Ge(100), in contrast to dative-bonded aliphatic amines. The [2 + 2] and [4 + 2] cycloaddition products of pyrrole and *N*-methylpyrrole are similarly affected by the loss of aromaticity, with binding energies approximately 24−29 kcal/mol weaker than those of the [2 + 2] and [4 + 2] cycloaddition products of the nonaromatic diene analogue of pyrrole, cyclopentadiene.[2] As a result, the dative-bonded and [2 + 2] cycloaddition products of pyrrole and *N*-methylpyrrole on Si(100) and Ge(100), as well as the [4 + 2] product on Ge(100), will not compete thermodynamically at room temperature even if their formation is kinetically favored.

This argument can explain why for *N*-methylpyrrole the [4 + 2] product is not observed at room temperature on the Ge(100) surface, where it reversibly desorbed. However, it cannot explain the lack of evidence for an EAS product for *N*-methylpyrrole on Ge(100), which is predicted to have a very long mean surface residence time ($\sim 1 \times 10^{16}$ h) at room temperature. Instead, the EAS product is probably not observed on Ge(100) for *N*-methylpyrrole because of an increased barrier relative to that on the Si(100) surface. We have previously reported that the barriers for most organic reactions on Ge(100) are significantly higher than on Si(100), an effect that is also observed in this study.[1,5,6] Although we have not calculated the barrier for EAS of *N*-methylpyrrole on Ge, the fact that some EAS products are observed for pyrrole and not for *N*-methylpyrrole on Ge suggests that a higher barrier for EAS may exist for *N*-methylpyrrole. A combination of thermodynamic and kinetic factors thus best explains the lack of observable products for *N*-methylpyrrole on Ge(100) at room temperature.

For the aromatic amines in this study, it is seen that the thermodynamics of competing reactions must be considered in order to account for their observed reactivity on the Si(100) and Ge(100) surfaces. This is in contrast to the aliphatic amines, whose reactivity on Si(100) and Ge(100) can be predicted on the basis of kinetic (and dynamic) factors alone because of the negligible rates of reversible desorption at room temperature of the reaction products.

C. Comparison of Molecular and Surface Reactivity of Pyrrole. Although the adsorption of many organic molecules has been investigated on clean semiconductor surfaces, there have been few in-depth analyses on how these systems compare to molecular organic reactions. Such comparisons may be valuable by determining whether trends and principles from molecular organic chemistry might also be applicable to understanding the reactivity of semiconductor surfaces. Because of its rich and extensively examined chemistry, pyrrole is an excellent probe molecule for addressing this issue. A comparison of the known molecular reactivity of pyrrole and its reactivity on the Si(100) and Ge(100) semiconductor surfaces is summarized in Table 2. We begin our discussion with a comparison of protonation and dative bonding of pyrrole and proceed down the Table.

Dative bonding and protonation of pyrrole can be considered to be analogous reactions. Both reactions involve an attack of the pyrrole ring by an electrophile, either H^+ in the molecular case or the electron-deficient down atom of the Si(100) or Ge(100) dimer in the surface case. As seen in this study, dative bonding of pyrrole is much less thermodynamically favorable in comparison to that of the aliphatic amines investigated. This result may have been predicted by considering the known lower basicity of pyrrole versus aliphatic amines. The explanations for the molecular and surface cases are the same: both dative bonding and protonation suffer energetically for pyrrole relative to aliphatic amines because of the accompanying loss of aromaticity.

Our calculations indicate that dative bonding at the α-C position on Si(100) is the most energetically favorable (−6.6 kcal/mol), followed by the β-C position (−4.1 kcal/mol). Dative bonding at the nitrogen of pyrrole (−0.6 kcal/mol) is the least thermodynamically favorable position. The order of thermodynamic favorability for dative bonding, α-C > β-C > N, is consistent with that observed for the protonation of pyrrole, where at equilibrium, protonation values at the β-C and nitrogen of pyrrole have been measured to be only ∼1% and ∼0.0001% of the value at the α-C, respectively.[39]

This agreement is insightful because it indicates that we can use the explanation given for the thermodynamic preference for the protonation of pyrrole to explain the thermodynamic preference for dative bonding at the α-C position of pyrrole on Si(100) and Ge(100). That is, the relative thermodynamic stability can be related to the number of resonance structures available following an attack by an electrophile. As shown in Figure 17, an attack by an electrophile (i.e., the down Si atom of the dimer) at the α-C position of pyrrole has three resonance forms, compared to two at the β-C position and only one at the nitrogen. Whereas dative bonding at all ring positions of pyrrole results in a loss of aromaticity and hence resonance energy, the resonance energy lost for pyrrole dative-bonded at the α-C is less because it retains more resonance forms than the other products.

The N−H dissociation reaction can be considered to be a surface analogue to proton transfer because both reactions result in the transfer of a hydrogen in exchange for another species at the nitrogen. We observed for the aromatic amines in this study a higher reactivity toward N−H dissociation on Ge(100) in comparison to that for the aliphatic amines. This result was explained by the alternative pathway available to pyrrole involving initial dative bonding at a ring carbon, which is

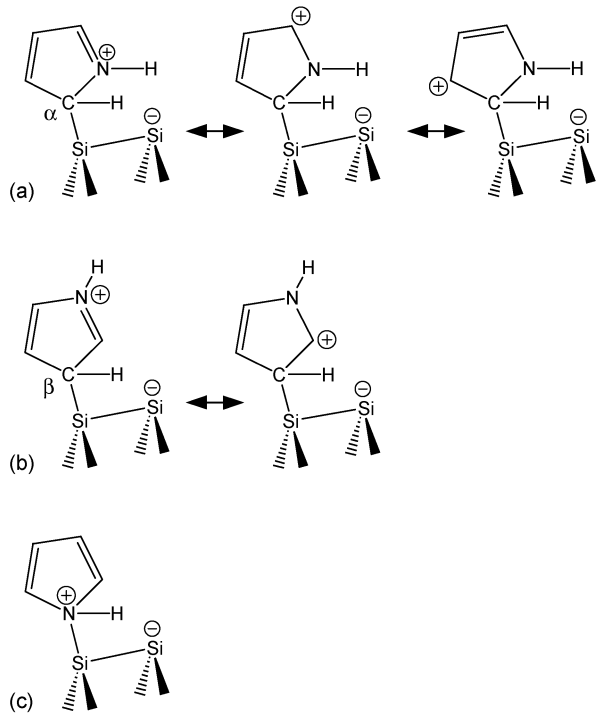

Figure 17. Resonance structures of pyrrole dative-bonded at the (a) α-C, (b) *β*-C, and (c) N atoms.

kinetically favorable to the direct N−H dissociation pathway. This behavior is mirrored in the molecular case by the higher acidity of aromatic amines versus aliphatic amines. For example, the pK_a values of pyrrole and pyrrolidine in DMSO are 23.0 and ∼44, respectively.[49]

The results of this study suggest that pyrrole (on Si and Ge) and *N*-methylpyrrole (on Si) both undergo some degree of electrophilic aromatic substitution (EAS) at a ring carbon. This is interesting because electrophilic substitution has not been previously reported for other aromatic molecules such as benzene and its derivatives (e.g., toluene) on Si(100)-2×1[8,40,50−57] and Ge(100)-2×1.[37] Again, a consideration of the molecular reactivity of pyrrole is useful for explaining this observation. Pyrrole is known to be much more reactive in general toward electrophilic substitution reactions than benzene because of its lower resonance energy, with the overall rate of proton exchange for deuterium in pyrrole-2,3,4,5-d_4 10^{15} times that for deuteriobenzene.[39] Thus, the observation of an EAS reaction for pyrrole and not for benzene or its derivatives on Si(100) and Ge(100) is consistent with the much faster rate for pyrrole that is observed in molecular organic chemistry.

Whereas some fraction of pyrrole molecules does appear to react via EAS on Si(100) and Ge(100), this work and previous studies performed on Si(100)[15,28] indicate that N−H dissociation is the major reaction pathway on both surfaces. This cannot be explained by the relative thermodynamics of the N−H dissociation product versus the EAS product because both adducts have binding energies that are more than sufficient for long-term room-temperature stability. Instead, the competition between N−H dissociation and EAS is governed by kinetic (and dynamic) rather than thermodynamic factors. As seen in the calculated potential energy surfaces in Figures 13 and 14, the pathway for N−H dissociation is indeed kinetically preferred over that for EAS, consistent with the observation of N−H dissociation as the major reaction pathway on Si and Ge. Again, this result exhibits similarities to and can be qualitatively predicted from the molecular reactivity of pyrrole because proton transfer at the nitrogen has been measured to be 10−100 times faster than at carbon.[39]

Thus, for all five cases in Table 2, there is a consistency between the trends observed for the molecular chemistry of pyrrole and the chemistry of pyrrole on clean semiconductor surfaces. We have provided through this comparison a strong demonstration that the trends and principles used to understand molecular organic reactivity can also be useful and applicable for understanding the reactivity of semiconductor surfaces. These results indicates that likening the Si(100)-2×1 and Ge(100)-2×1 surfaces to ordered arrays of electrophile/nucleophile pairs represents a valid description of the chemical reactivity of these surfaces rather than just a superficial construct. The similar molecular and surface chemistry of pyrrole also provides a convincing mechanistic indication that the N−H dissociation and electrophilic substitution reactions do indeed involve proton transfer to the surface rather than homolytic bond cleavage, a point that has been previously argued for N−H dissociation of other amines and the ene reaction of various ketones on Si(100) and Ge(100).[1,3−6]

V. Conclusions

Therefore, to better understand the fundamental chemistry of the Ge(100) surface with organic molecules, we have examined its reaction with a model system of six cyclic, five-membered aliphatic and aromatic amines using multiple internal reflection infrared spectroscopy in combination with DFT cluster calculations. The reactions of pyrrolidine, *N*-methylpyrrolidine, pyrrole, and *N*-methylpyrrole were then probed on the Si(100)-2×1 surface for comparison.

For the four aliphatic amines in this study, dative bonding of the N lone pair to the electrophilic down atom of the surface dimer is a barrierless process that competes to form metastable surface adducts that are observed as the majority product at room temperature on the Ge(100) surface. Interestingly, at higher coverages, some evidence for N−H dissociation is seen on Ge(100). On the Si(100) surface, the tertiary aliphatic amines also become trapped in the dative-bonded state, whereas the secondary aliphatic amines proceed from the dative-bonded precursor state to undergo N−H dissociation at room temperature. The presence of the alkene bond in 3-pyrroline is calculated to have an insignificant effect on the energetics of the N−H dissociation reaction. The lack of a significant amount of the [2 + 2] cycloaddition product for 3-pyrroline on Ge(100) can be explained by unfavorable kinetic competition, and indeed the reactions of all of the aliphatic amines in this study on both the Si(100) and Ge(100) surfaces can be understood by recognizing that they are under kinetic control at room temperature.

For the aromatic amines investigated, thermodynamic factors in addition to kinetic and dynamic factors also play a major role in determining their reactivity on semiconductor surfaces. One such effect is the destabilization of reaction products that require a loss of aromaticity (e.g., dative-bonded and cycloaddition adducts), which may lead to the elimination of such products at room temperature via rapid, reversible desorption. The delocalized system of π electrons also allows a kinetically more favorable, alternative pathway for N−H dissociation via dative bonding at a ring carbon rather than at the nitrogen. This results in the facile N−H dissociation of pyrrole on the Ge(100) surface, in contrast to the case for aliphatic amines, where most of the molecules remained trapped in the dative-bonded precursor state. Interestingly, the IR experiments and theoretical calculations indicate that pyrrole and *N*-methylpyrrole undergo

some degree of electrophilic aromatic substitution at the surfaces, a reaction that has not been previously observed for benzene and other aromatic molecules.

The known molecular reactivity of pyrrole and its observed and calculated reactivity on Si(100)-2×1 and Ge(100)-2×1 were found to be surprisingly consistent. This similarity indicates that principles and trends used to understand molecular organic chemistry may also be used to understand bonding at semiconductor surfaces. From this comparison, we can conclude that the Si(100)-2×1 and Ge(100)-2×1 surfaces may be portrayed as arrays of individual chemical units that can undergo localized reactions (e.g., proton transfer) that not only form adducts analogous to molecular organic chemistry products but from which mechanistic pathways may be inferred from their molecular organic reaction analogues.

Acknowledgment. G.T.W. and M.A.F. acknowledge financial support from National Science Foundation Graduate Fellowships. S.F.B. acknowledges financial support from the National Science Foundation (DMR 9896333; CHE 9900041) and from the Beckman Foundation. S.F.B. is a Camille Dreyfus Teacher-Scholar. C.B.M. thanks the Charles Powell Foundation for funding. J.F.T. acknowledges support from the Vice Provost for Undergraduate Education at Stanford University.

References and Notes

(1) Wang, G. T.; Mui, C.; Musgrave, C. B.; Bent, S. F. *J. Am. Chem. Soc.* **2002**, *124*, 8990.
(2) Wang, G. T.; Mui, C.; Musgrave, C. B.; Bent, S. F. *J. Phys. Chem. B* **1999**, *103*, 6803.
(3) Wang, G. T.; Mui, C.; Musgrave, C. B.; Bent, S. F. *J. Phys. Chem. B* **2001**, *105*, 3295.
(4) Mui, C.; Wang, G. T.; Bent, S. F.; Musgrave, C. B. *J. Chem. Phys.* **2001**, *114*, 10170.
(5) Wang, G. T.; Mui, C.; Musgrave, C. B.; Bent, S. F. *J. Phys. Chem. B* **2001**, *105*, 12559.
(6) Mui, C.; Han, J. H.; Wang, G. T.; Musgrave, C. B.; Bent, S. F. *J. Am. Chem. Soc.* **2002**, *124*, 4027.
(7) Kugler, T.; Thibaut, U.; Abraham, M.; Folkers, G.; Gopel, W. *Surf. Sci.* **1992**, *260*, 64.
(8) Bitzer, T.; Alkunshalie, T.; Richardson, N. V. *Surf. Sci.* **1996**, *368*, 202.
(9) Bitzer, T.; Richardson, N. V. *Appl. Phys. Lett.* **1997**, *71*, 662.
(10) Armstrong, J. L.; Sun, Y. M.; White, J. M. *Appl. Surf. Sci.* **1997**, *120*, 299.
(11) Liu, H. B.; Hamers, R. J. *Surf. Sci.* **1998**, *416*, 354.
(12) Rummel, R. M.; Ziegler, C. *Surf. Sci.* **1998**, *418*, 303.
(13) Zhu, X. Y.; Mulder, J. A.; Bergerson, W. F. *Langmuir* **1999**, *15*, 8147.
(14) Mulcahy, C. P. A.; Carman, A. J.; Casey, S. M. *Surf. Sci.* **2000**, *459*, 1.
(15) Qiao, M. H.; Cao, Y.; Deng, J. F.; Xu, G. Q. *Chem. Phys. Lett.* **2000**, *325*, 508.
(16) Bitzer, T.; Richardson, N. V.; Reiss, S.; Wuhn, M.; Woll, C. *Surf. Sci.* **2000**, *458*, 173.
(17) Cao, X. P.; Hamers, R. J. *J. Am. Chem. Soc.* **2001**, *123*, 10988.
(18) Luo, H. B.; Lin, M. C. *Chem. Phys. Lett.* **2001**, *343*, 219.
(19) Kong, M. J.; Lee, K. S.; Lyubovitsky, J.; Bent, S. F. *Chem. Phys. Lett.* **1996**, *263*, 1.
(20) Hohenberg, P.; Kohn, W. *Phys. Rev. B* **1964**, *136*, 864.
(21) Kohn, W.; Sham, L. J. *Phys. Rev. A* **1965**, *140*, 1133.
(22) Mui, C. Ph.D. Thesis, Stanford University: Stanford, CA, 2003.
(23) Widjaja, Y.; Musgrave, C. B. *Surf. Sci.* **2000**, *469*, 9.
(24) Frisch, M. J.; Trucks, G. W.; Schlegel, H. B.; Scuseria, G. E.; Robb, M. A.; Cheeseman, J. R.; Zakrzewski, V. G.; Montgomery, J. A., Jr.; Stratmann, R. E.; Burant, J. C.; Dapprich, S.; Millam, J. M.; Daniels, A. D.; Kudin, K. N.; Strain, M. C.; Farkas, O.; Tomasi, J.; Barone, V.; Cossi, M.; Cammi, R.; Mennucci, B.; Pomelli, C.; Adamo, C.; Clifford, S.; Ochterski, J.; Petersson, G. A.; Ayala, P. Y.; Cui, Q.; Morokuma, K.; Malick, D. K.; Rabuck, A. D.; Raghavachari, K.; Foresman, J. B.; Cioslowski, J.; Ortiz, J. V.; Stefanov, B. B.; Liu, G.; Liashenko, A.; Piskorz, P.; Komaromi, I.; Gomperts, R.; Martin, R. L.; Fox, D. J.; Keith, T.; Al-Laham, M. A.; Peng, C. Y.; Nanayakkara, A.; Gonzalez, C.; Challacombe, M.; Gill, P. M. W.; Johnson, B. G.; Chen, W.; Wong, M. W.; Andres, J. L.; Head-Gordon, M.; Replogle, E. S.; Pople, J. A. *Gaussian 98*, revision A.5; Gaussian, Inc.: Pittsburgh, PA, 1998.
(25) Becke, A. D. *Phys. Rev. A* **1988**, *38*, 3098.
(26) Lee, C. T.; Yang, W. T.; Parr, R. G. *Phys. Rev. B* **1988**, *37*, 785.
(27) Becke, A. D. *J. Chem. Phys.* **1993**, *98*, 5648.
(28) Cao, X.; Coulter, S. K.; Ellison, M. D.; Liu, H.; Liu, J.; Hamers, R. J. *J. Phys. Chem. B* **2001**, *105*, 3759.
(29) Krueger, P. J.; Jan, J. *Can. J. Chem.* **1970**, *48*, 3236.
(30) Billes, F.; Geidel, E. *Spectrochim. Acta, Part A* **1997**, *53*, 2537.
(31) Chabal, Y. J. *Surf. Sci.* **1986**, *168*, 594.
(32) Queeney, K. T.; Chabal, Y. J.; Raghavachari, K. *Phys. Rev. Lett.* **2001**, *86*, 1046.
(33) Teplyakov, A. V.; Lal, P.; Noah, Y. A.; Bent, S. F. *J. Am. Chem. Soc.* **1998**, *120*, 7377.
(34) Lal, P.; Teplyakov, A. V.; Noah, Y.; Kong, M. J.; Wang, G. T.; Bent, S. F. *J. Chem. Phys.* **1999**, *110*, 10545.
(35) Mui, C.; Bent, S. F.; Musgrave, C. B. *J. Phys. Chem. A* **2000**, *104*, 2457.
(36) Fink, A.; Huber, R.; Widdra, W. *J. Chem. Phys.* **2001**, *115*, 2768.
(37) Fink, A.; Menzel, D.; Widdra, W. *J. Phys. Chem. B* **2001**, *105*, 3828.
(38) Widjaja, Y.; Musgrave, C. B. To be submitted for publication.
(39) Jackson, A. H. In *Reactivity of the 1H-Pyrrole Ring System*; Jones, R. A., Ed.; Wiley & Sons: New York, 1990; Vol. 48, p 295.
(40) Coulter, S. K.; Hovis, J. S.; Ellison, M. D.; Hamers, R. J. *J. Vac. Sci. Technol., A* **2000**, *18*, 1965.
(41) Wolkow, R. A. *Ann. Rev. Phys. Chem.* **1999**, *50*, 413.
(42) Hamers, R. J.; Coulter, S. K.; Ellison, M. D.; Hovis, J. S.; Padowitz, D. F.; Schwartz, M. P.; Greenlief, C. M.; Russell, J. N. *Acc. Chem. Res.* **2000**, *33*, 617.
(43) Bent, S. F. *J. Phys. Chem. B* **2002**, *106*, 2830.
(44) Bent, S. F. *Surf. Sci.* **2002**, *500*, 879.
(45) Buriak, J. M. *Chem. Rev.* **2002**, *102*, 1271.
(46) Liu, Q.; Hoffmann, R. *J. Am. Chem. Soc.* **1995**, *117*, 4082.
(47) Choi, C. H.; Gordon, M. S. *J. Am. Chem. Soc.* **1999**, *121*, 11311.
(48) Lu, X.; Xu, X.; Wang, N. Q.; Zhang, Q.; Lin, M. C. *J. Phys. Chem. B* **2001**, *105*, 10069.
(49) Bordwell, F. G.; Drucker, G. E.; Fried, H. E. *J. Org. Chem.* **1981**, *46*, 632.
(50) Lopinski, G. P.; Moffatt, D. J.; Wolkow, R. A. *Chem. Phys. Lett.* **1998**, *282*, 305.
(51) Lopinski, G. P.; Fortier, T. M.; Moffatt, D. J.; Wolkow, R. A. *J. Vac. Sci. Technol., A* **1998**, *16*, 1037.
(52) Gokhale, S.; Trischberger, P.; Menzel, D.; Widdra, W.; Droge, H.; Steinruck, H. P.; Birkenheuer, U.; Gutdeutsch, U.; Rosch, N. *J. Chem. Phys.* **1998**, *108*, 5554.
(53) Borovsky, B.; Krueger, M.; Ganz, E. *Phys. Rev. B* **1998**, *57*, R4269.
(54) Kong, M. J.; Teplyakov, A. V.; Lyubovitsky, J. G.; Bent, S. F. *Surf. Sci.* **1998**, *411*, 286.
(55) Borovsky, B.; Krueger, M.; Ganz, E. *J. Vac. Sci. Technol., B* **1999**, *17*, 7.
(56) Kong, M. J.; Teplyakov, A. V.; Jagmohan, J.; Lyubovitsky, J. G.; Mui, C.; Bent, S. F. *J. Phys. Chem. B* **2000**, *104*, 3000.
(57) Qiao, M. H.; Cao, Y.; Tao, F.; Liu, Q.; Deng, J. F.; Xu, G. Q. *J. Phys. Chem. B* **2000**, *104*, 11211.